UNIVERSITY OF CALIFORNIA, SAN DIEGO

Type 2A Protein Phosphatases mediate Abscisic Acid Responses by interacting with the protein kinase Open Stomata 1

A Thesis submitted in partial satisfaction of the requirements
for the degree Master of Science

in

Biology

by

Bianca Manalansan

Committee in charge:

Professor Julian Schroeder, Chair
Professor Nigel Crawford
Professor Mark Estelle
Professor Yunde Zhao

2013

The Thesis of Bianca Manalansan is approved and it is acceptable in quality and form for publication on microfilm and electronically:

Chair

University of California, San Diego

2013

TABLE OF CONTENTS

LIST OF FIGURES AND TABLES

ACKNOWLEDGEMENTS

I thank Dr. Julian Schroeder for the opportunity to be a part of his laboratory and research for the past two years. Our regular lab meetings and research discussions gave me valuable research advice and guidance for my project. Without Dr. Schroeder, the experiences and memories I have gained here would not have been possible. Furthermore, I greatly appreciate his support as chair of my committee. My thanks extend to my committee members, Drs. Nigel Crawford, Mark Estelle and Yunde Zhao, for taking the time to serve on my committee.

My most sincere gratitude goes to my mentor, Rainer Waadt. I have learned so much from him the past year and I do not think my M.S. degree would have been possible without him. I thank him for his patience, kindness, understanding, inspiration, and for believing in me to carry out my project. Learning from his work ethic, I have also learned how to become a harder and smarter worker in the lab. I could not imagine having a better mentor for my M.S. degree. He has taught me more than I could have ever hoped for.

I would also like to express my thanks to rest of the Schroeder Lab members for helping me with problems and questions along the way. Being a part of the Schroeder laboratory has made a positive impact in my life and for that, I thank all of the members of the lab for playing a part in this.

Finally, for the constant support from my best friends, boyfriend, and family that made this possible.

ABSTRACT OF THE THESIS

Type 2A Protein Phosphatases mediate Abscisic Acid Responses by interacting with the protein kinase Open Stomata 1

by

Bianca Manalansan

Master of Science in Biology

University of California, San Diego, 2013

Professor Julian Schroeder, Chair

The plant hormone abscisic acid (ABA) controls the water status of plants by regulating many physiological processes including seed germination, root growth and stomatal movements. However, the molecular mechanisms of ABA signaling have yet to be fully understood. Here, the involvement of Type 2A protein phosphatases (PP2As) in

ABA signaling has been studied. To functionally characterize *Arabidopsis* PP2As, subcellular localization and protein-protein-interaction analyses of PP2As were performed. These analyses revealed that all PP2AAs and PP2ACs are localized in the cytoplasm and the nucleus and can form complexes among each other in the cytoplasm, however with varying interaction strength. Phenotypical assays with *pp2a* double mutant combinations revealed an ABA hyposensitivity during seed germination, but ABA hypersensitivity during root growth and no altered response during ABA-induced stomatal closure. These ABA responses could be linked to the physical interaction of PP2As with the protein kinase OST1, which is part of the core ABA signaling pathway.

1. INTRODUCTION

Protein phosphorylation is an important molecular switch in biological signaling networks. The counteracting activities of protein kinases and phosphatases determine the phosphorylation status of the target protein therefore affecting its function, subcellular localization, activity, and stability (Moorhead et al., 2009). Protein phosphatase type 2A (PP2A) is one of the most abundant types of serine/threonine phosphatases in eukaryotic cells (Cohen, 1997; Kremmer et al., 1997) and highly conserved in its sequence and functional properties (Moorhead et al., 2009). PP2As are heterotrimeric holoenzyme complexes consisting of regulatory PP2AA- and PP2AB- and catalytic PP2AC-subunits (Xu et al., 2006; Shi, 2009). The PP2AA-subunits act as a scaffolding subunit whereas the PP2AB-subunits are thought to be involved in subcellular targeting and substrate specificity of PP2As (DeLong, 2006; Farkas et al., 2007; Xu et al., 2006; Shi et al., 2009). The Arabidopsis genome encodes for three PP2AA-subunits (65-kDa), seventeen PP2AB-subunits subdivided into two B-(55 kDa), nine B'-(54-74 kDa), five B''-(72-130 kDa) subunits and TONNEAU2/FASS (TON2), and five PP2AC-subunits (36 kDa) (DeLong, 2006; Farkas et al., 2007) with a potential of 255 possible holoenzyme complexes. Forward and reverse genetics approaches revealed functional roles of PP2As in ABA signaling (Kwak et al., 2002; Pernas et al., 2007) in regulation of auxin fluxes (Fischer et al., 1996; Gabers et al., 1996; Rashotte et al., 2001; Michniewicz et al., 2007; Ballesteros et al., 2012; Dai et al., 2012), brassinosteroid signaling (Tang et al., 2010; Wu et al., 2011), ethylene signaling and biosynthesis (Larsen and Cancel, 2003; Skottke et al., 2011), methyl jasmonate signaling (Saito et al., 2008; Trotta et al., 2011) blue light signaling (Tseng and Briggs, 2010) and microtubule organization (McClinton and Sung, 1997; Camilleri et al., 2002; Kirik et al., 2012).

Arabidopsis PP2AA isoforms RCN1 (Root Curl in NPA), PP2AA2, and PP2AA3 are cytoplasmic and nuclear proteins (Blakeslee et al., 2008; Tran et al., 2012) that consist of 15 tandem HEAT-repeats, forming a hook-like structure for binding to the PP2AC- and PP2AB-subunits (Farkas et al., 2007; Xu et al., 2006). The PP2AAs have important regulatory functions. Binding of PP2AAs to the PP2ACs alters their kinetic properties by enabling a fully activated PP2AC conformation (Price and Mumby, 2000). Further as a scaffolding subunit, PP2AAs allow the interaction of the PP2ACs and PP2ABs (Ruediger et al., 1994; Xu et al., 2006). *RCN1* was originally discovered as a regulator of auxin transport and gravitropsim by regulating the polarity of the PIN-type auxin transporter subcellular localization (Garbers et al., 1996; Rashotte et al., 2001; Michniewicz et al., 2007). Recently, it has been shown that PP2AA subunits form complexes with PP6 catalytic subunits FyPP1 and FyPP3 to direct auxin fluxes by dephosphorylation of PIN proteins (Dai et al., 2012). *rcn1* mutant seedlings display abnormalities in cell division patterns and reduced growth under ionic, osmotic, and oxidative stress conditions at the root apical meristem (Blakeslee et al., 2008). *RCN1*, also found in a forward genetic screen for *enhanced ethylene response 1 (eer1)* is involved in ethylene biosynthesis by regulating the turnover of ethylene biosynthesis genes (Larsen and Cancel, 2003; Zhou et al., 2004; Muday et al., 2006; Skottke et al., 2011). *RCN1* has also been found to play an important role in blue light signaling by down-regulating the blue light-activated *PHOT2* blue light receptor (Tseng and Briggs, 2010). Reverse genetics approaches also revealed functional roles of RCN1 in abscisic acid (ABA) and methyl jasmonate (MeJA) signaling (Kwak et al., 2002; Saito et al., 2008). In the ecotype Wassilewskija, *rcn1* mutation resulted in an ABA and MeJA

insensitivity phenotype in seed germination and stomatal closure (Kwak et al., 2002; Saito et al., 2008). Neither MeJA nor ABA induced reactive oxygen species (ROS) production, inward rectifying potassium channel inhibition, and stomatal closure in the *rcn1* mutant (Saito et al., 2008). Furthermore, *rcn1* mutation impaired ABA activation of slow anion channels and displayed a reduced sensitivity of ABA induced cytosolic calcium increases (Kwak et al., 2002). These data suggested that RCN1 functions high upstream in the ABA signaling pathway (Kwak et al., 2002; Saito et al., 2008). Severe phenotypic defects, which include abnormal embryogenesis, dwarfism, and sterility are observed in PP2AA double mutants in combinations of *rcn1* with either *pp2aa2* or *pp2aa3,* indicating that RCN1 plays a major role in the regulation of PP2A activity (Zhou et al., 2004; Michniewicz et al., 2007). The functions of PP2AA2 and PP2AA3 are revealed only when RCN1 is absent. The key function of RCN1 has yet to be fully understood, but data suggests that gene dosages of PP2AAs are an important determinant of PP2A function rather than tissue specificity of PP2AA expression (DeLong, 2006; Zhou et al., 2004).

Though *Arabidopsis* PP2ABs, as in other eukaryotes, are important for substrate specificity and cellular localization (Farkas et al., 2007), the function of most PP2ABs is still unclear. Not much is known about the two *Arabidopsis* PP2AB-subunits or the PP2AB''-subunits. PP2ABalpha and PP2ABbeta carry five degenerate WD-40 repeats and have 48% amino acid sequence identity with animal PP2ABs (Corum et al., 1996). The five *Arabidopsis* PP2AB''-subunits carry calcium binding EF-hand motifs with TON2 representing a PP2AB''-like subunit (Farkas et al., 2007). The most well known of the PP2AB isoforms are the PP2AB'-subunits (Terol et al., 2002; Matre et al., 2009;

Eichorn et al., 2009). Despite a high degree of conservation, plant and animal PP2AB'-subunits have evolved completely independently (Terol et al., 2002). Sequence comparison of *Arabidopsis* PP2AB'-subunits displayed a highly conserved central domain with diverged amino- and carboxy- terminal regions (Terol et al., 2002). This central region again supports the important role for the assembly of PP2AB'-subunits with the heterotrimeric PP2A complex for substrate specificity and cellular localization (Depaoli-Roach et al., 1994; Terol et al., 2002). Early studies identified PP2AB'-subunits as being similar proteins that are expressed ubiquitously in *Arabidopsis* organs (Haynes et al., 1999; Terol et al., 2002). The *PP2AB'gamma* gene has alternatively spliced transcripts and accumulates in response to heat stress, proposing this subunit could be involved in stress response mechanisms in plants (Haynes et al., 1999). Interestingly, transcripts of PP2AB'alpha, -B'beta and -B'delta subunits do not fluctuate in response to heat shock (Terol et al., 2002).

The subcellular localization of PP2AB'subunits is diverse. Depending on the orientation of the fluorescent protein tag PP2AB'gamma, -B'zeta, -B'eta and -B'theta were found in the nucleus and cytosol but also in the nucleolus (PP2AB'eta), in peroxisomes (PP2AB'theta), or in the mitochondria (PP2AB'zeta) (Matre et al., 2009). These findings support that the different PP2AB' isoforms could function in unique subcellular localizations of PP2A complexes (Latorre et al., 1997; Terol et al., 2002).

Recent data have shown that PP2As dephosphorylate BZR1, a transcription factor involved in brassinosteroid signaling, and that BZR1 directly interacts with several PP2AB'-isoforms (Tang et al., 2011). Phenotypic defects of *pp2ab'alpha/pp2ab'beta*

double mutants, lacking the two major BZR1-binding PP2AB′-isoforms, displayed severe dwarfism and reduced plant growth (Tang et al., 2011). TON2/FASS has been shown to interact with the catalytic PP2ACs in yeast-two-hybrid assays and is involved in the control of cytoskeletal structures in plants (Camilleri et al., 2002). The *ton2/fass* mutation causes abnormalities in microtubule assembly and disrupts mechanisms involved in cell elongation and cell division (Fischer et al., 1996; McClinton and Sung, 1997; Camilleri et al., 2002; Kirik et al., 2012).

The five catalytic PP2AC-subunits in *Arabidopsis* are phylogenetically separated into two groups, subfamily I (PP2AC1, PP2AC2, and PP2AC5) and subfamily II (PP2AC3 and PP2AC4) (Casamayor et al., 1994). The PP2ACs share 95% sequence identity within a given subfamily and 80% between the two subfamilies (Ballesteros et al., 2012). All *PP2AC* genes are expressed in all organs with varying levels of expression (Ariño et al., 1993). The C-terminal TPDYFL tail of PP2ACs is highly conserved and T- and Y-phosphorylation has been reported in human cells to inhibit PP2A activity (reviewed in Sents et al., 2012). In addition, reversible methylation of PP2ACs at their last L residue is important for PP2A activity and holoenzyme assembly/biogesesis (reviewed in Sents et al., 2012). There is only limited knowledge about the functional roles of PP2ACs. Silencing of a subfamily of tomato *PP2AC* genes caused enhanced response to bacterial avirulence proteins and localized cell death in stems and leaves suggesting potential roles for PP2As in defense mechanisms (He et al., 2004). Recently, it has been revealed that PP2AC3 and PP2AC4 catalytic subunits have important functions in auxin distrribution in the root (Ballesteros et al., 2012), whereas a *pp2ac5*

mutant showed a reduced response to brassinazole (Tang et al., 2011). The loss of function mutant *pp2ac2* was found to be hypersensitive to ABA in developmental processes such as lateral- and primary root growth, seedling development, germination, seed dormancy, and responses to drought and high salt and sugar stresses (Pernas et al., 2007). *pp2ac2* mutants displayed delayed seed germination and increased dormancy in response to ABA, while *PP2AC2* overexpression resulted in earlier seed germination and cotyledon expansion when compared to wild type Wassilewskija (Pernas et al., 2007). It was proposed that *PP2AC2* plays a specific role as a negative regulator of ABA signaling by regulation of ABA dependent gene expression (Pernas et al., 2007). However while *pp2ac2* displays ABA hypersensitivity during seed germination, *rcn1* was ABA hyposensitive (Kwak et al., 2002; Pernas et al., 2007) indicating that PP2AA- and PP2AC- subunits have contrasting functions during ABA inhibition of seed germination.

The phytohormone ABA is crucial for the regulation of seed germination, root development, flowering, and stomatal movements (Acharya et al., 2009; Himmelbach et al., 1998; De Smet et al., 2006; Finkelstein et al., 2008; Kim et al., 2010; Santner et al., 2009). Furthermore, ABA promotes root growth inhibition and seed dormancy during abiotic stress (Deak and Malamy, 2005; Rodriguez-Gacio et al., 2009; Duan et al., 2013). ABA synthesis is activated by high salinity stress and drought, stimulating stomatal closure to protect plants from dehydration (Wilkinson and Davies, 2002). PYRABACTIN RESISTANCE 1 (PYR1)/ PYR1 LIKE (PYL)/ REGULATORY COMPONENT OF ABA RECEPTOR (RCAR), in-short PYLs, are members of a protein family that can bind to ABA (Ma et al., 2009; Park et al., 2009; Santiago et al., 2009). The ABA-PYL

complexes can interact with and negatively regulate Clade A TYPE 2C PROTEIN PHOSPHATASES (PP2Cs) (Park et al., 2009; Ma et al., 2009; Santiago et al., 2009; Nishimura et al., 2010). PP2C inhibition allows the activation of SNF1-RELATED KINASES 2 (SnRK2s) (Fujii et al., 2009; Umezawa et al., 2009; Vlad et al., 2009), which can target transcription factors, ion channels responsible for stomatal closure, and NADPH oxidases (Kobayashi et al., 2005; Furihata et al., 2006; Geiger et al., 2009; Lee et al., 2009; Sato et al., 2009; Sirichandra et al., 2009, 2010; Brandt et al., 2012).

In an effort to functionally characterize the *Arabidopsis* PP2As, subcellular localization analyses were performed for all PP2AAs and PP2ACs and for nine out of seventeen PP2ABs. Protein-protein-interaction analyses using BiFC and yeast-two-hybrid assays established an interaction network of PP2AAs and PP2ACs supporting that all PP2AAs and PP2ACs can form complexes, however with varying interacting strengths. Phenotypical analyses using *pp2a* double mutant combinations revealed that these mutants are hyposensitive to ABA during seed germination but hypersensitive to ABA in root growth. However, none of the mutants analyzed displayed a phenotype for ABA induced stomatal closure. The involvement of PP2As in ABA signaling could be linked to the physical interactions of PP2AAs and PP2ABs with the protein kinase OST1 which is a component of the core ABA signaling network.

2. RESULTS

2.1. Subcellular localization of PP2A subunits

To analyze the subcellular localization of the PP2As, PP2AAs and PP2ABs were cloned into plant compatible vectors with the fluorescent protein (FP) mTurquoise (mT) fused to the PP2A N-terminus or mVenus fused to the PP2A C-terminus (Fig 1). The PP2AC C-terminal TPDYFL tail is highly conserved and methylation of the last L residue is important for PP2A activity and holoenzyme assembly (Sents et al., 2012). Therefore, PP2ACs were fused with mVenus at their N-terminus. Constructs were transiently expressed by *Agrobacterium* infiltration into epidermal cells of *N. benthamiana* and examined by fluoresence microscopy, as shown by maximum projections of z-stacks (Fig 1). mTurquoise-PP2AA (Fig 1a-c) and PP2AA-mVenus (Fig 1d-f) exhibited strong fluorescence in the cytoplasm and nucleus while mVenus-PP2ACs localized in the cytoplasm, nucleus, and in cellular dots (Fig 1m-q). Compared to the PP2AAs and PP2ACs, the PP2ABs had more specific subcellular localizations (Fig 1g-l and Fig S1). Also expression in *N. benthamiana* was weak for PP2ABs, probably due to toxic effects as seen by necrosis on *N. benthamiana* leaves (data not shown). In initial experiments to localize PP2AB-FP fusions were performed using the pUBQ10 promoter for expression control. Later, a β-Estradiol inducible system (Schlucking et al., 2013) was used to express PP2AB-FPs, which reduced toxic effects of PP2ABs on *N. benthamiana* leaves and improved expression. Using these systems, PP2AB'alpha and PP2AB'beta fusion proteins were localized in the nucleus and in cytoplasmic strains (Fig 1g,h,j,k). mT-PP2AB'delta was localized in the cytoplasm (Fig 1i) whereas PP2AB'delta-mVenus was found in the plasma membrane and in dot like structures (Fig 1l). PP2ABalpha and PP2AB'gamma were found in the cytoplasm (Fig S1a,b,f,g) while mT-PP2ABalpha and

mT-PP2AB'gamma labeled net/mesh like structures in the cytoplasm (Fig S1a,b). mT-PP2AB'epsilon localized in the cytoplasm and nucleus (Fig S1c) while PP2AB'epsilon-mVenus was found in micro-domains of the plasma membrane (Fig S1h). mT-PP2AB'zeta could not be expressed and mT-PP2AB'eta and mT-PP2AB'theta localized in the nucleolus, nucleus, and cytoplasm (Fig S1d,e). PP2AB'zeta, PP2AB'eta, and PP2AB'theta-mVenus were identified in the nucleus, nucleolus and in dot like structures (Fig S1i-k) with PP2AB'eta-mVenus displaying also strong fluorescence at the plasma membrane (Fig S1j). The investigation of PP2A localizations raised the question about the localization and interaction of PP2A complexes *in planta,* which has not yet been reported (Ballesteros et al., 2012).

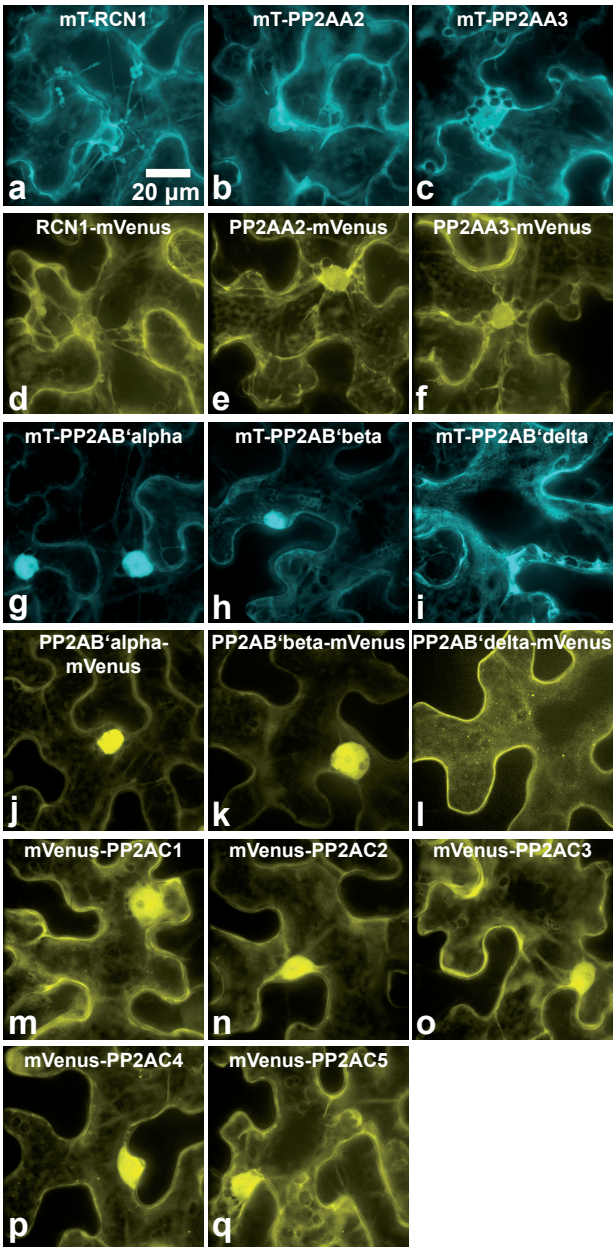

Figure 1. Subcellular localization of PP2A subunits. PP2A constructs were infiltrated into *N. benthamiana* leaves and expressed as an mTurquoise-(mT)-PP2A (cyan) or a PP2A-mVenus fusion (yellow). Three days after infiltration 32-z-stack images were recorded, displayed as a maximum projection. The fusion proteins analyzed in images **a-q** and the scale bar is indicated. **a-f**, PP2AAs are localized in the cytoplasm and the nucleus. **g-l,** PP2AB'alpha and PP2AB'beta are localized in the nucleus and in the cytoplasm, mT-PP2AB'delta is localized in the cytoplasm and PP2AB'delta-mVenus is localized at the plasma membrane and in dot-like structures. **m-q**, PP2ACs are localized in the cytoplasm, the nucleus and in dot-like structures.

2.2. PP2AAs and PP2ACs interact *in planta*

Bimolecular fluorescence complementation (BiFC) assays (Waadt et al., 2008) were used to study protein-protein interactions among PP2AAs and PP2ACs. BiFC depends on the formation of a fluorescent protein complex by two non-fluorescent fragments of the yellow fluorescent protein (YN, YFP N-terminal fragment; YC, YFP C-terminal fragment) when brought together by the interaction of two proteins fused to the fragments. The stable complex formation allows the detection of weak and/or transient protein interactions as well as simultaneously determining the subcellular localization of the protein interactions (Kerppola, 2006). In this experiment, YN-PP2As were transiently co-expressed with YC-PP2ACs into *N. benthamiana* epidermal cells by *Agrobacterium* infiltration, and the subcellular localization and YFP emission of reconstituted complexes were analyzed by confocal microscopy (Fig 2). Complexes of PP2AA1 (RCN1)–PP2AACs (Fig 2a-e), PP2AA2-PP2ACs (Fig 2f-j), and PP2AA3-PP2ACs (Fig 2k-o) exhibited a cytoplasmic fluorescence pattern as seen by the absence of fluorescence in the nucleus and by fluorescence in cytoplasmic strains. Quantification of the reconstituted YFP emission revealed that PP2AC1-PP2AC4 interact strongest with RCN1, while PP2AC3 also interacted strong with PP2AA2 (Fig 2,p,q). PP2AC5 exhibited strongest interaction with PP2AA3 (Fig 2r).

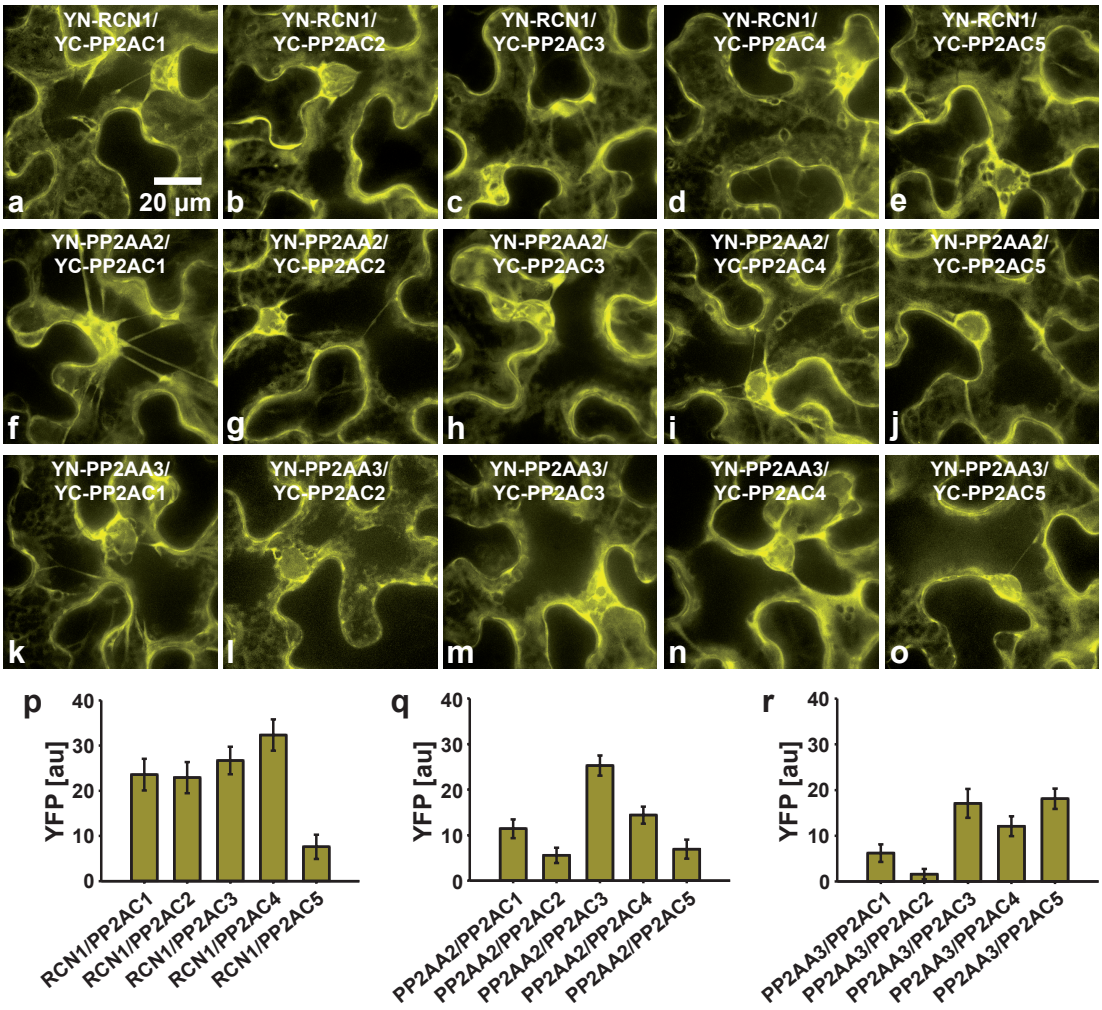

Figure 2. BiFC analyses of PP2AA interaction with PP2ACs. PP2AAs were fused to the YFP N-terminal fragment (YN-PP2AA) and PP2ACs were fused to the YFP C-terminal fragment (YC-PP2AC) and co-expressed in *N. benthamiana*. Images were acquired three days after transformation. **a-o**, Maximum projections of 32-z-stack-images showing the sub-cellular localizations of indicated PP2AA-PP2AC complexes in the cytoplasm. **p-r**, Semi-quantitative analyses of reconstituted YFP emission of indicated PP2AA-PP2AC BiFC combinations. Given are averages ± s.e.m of ten images.

2.3. PP2AAs and PP2ACs interact in yeast-two-hybrid analyses

The interaction of RCN1 and PP2AA2 with PP2ACs was also analyzed by yeast-two-hybrid assays (Fig 3). The two-hybrid system relies on the reconstitution of the activator domain (AD) and the DNA binding domain (BD) of the GAL4 transcription factor, which induces a reporter gene expression, often an auxotrophic marker (Fields et al 1994). RCN1 and PP2AA2 were cloned in fusion to the GAL4 AD into the vector pGAD.GH and all five PP2AC subunits were fused to the GAL4 BD in the vector pGBT9.BS (Fig 3). AD-RCN1, AD-PP2AA2, and BD-PP2AC constructs were transformed into PJ69-4A yeast strain and dilution series were spotted on SD-LW control media (Fig 3a,c) or on SD-LWH media for selection of interaction (Fig 3b,d). Also compilations of empty vectors and AD-RCN1, AD-PP2AA2 and BD-PP2ACs in combination with empty vectors were used as negative/transactivation controls. As seen in Fig 3b, RCN1 interacts with all five PP2AC subunits, however strongest interaction was found with PP2AC4, which was consistent with BiFC analysis (Fig 2p). In Fig 3d, PP2AA2 interacts with all five PP2AC subunits, however the interactions were weaker compared to RCN1, as indicated by longer growth of the yeast (7 days compared to 5 days) (Fig 3). PP2AA2 interacted strongest with PP2AC2-C4. pGAD.GH-AKT1 and pGBT9.BS-CIPK23 interaction was used as a positive control (Xu et al., 2006) displaying slightly more yeast growth-stronger interaction-when compared to PP2AA2-PP2AC interactions (Fig 3d). Combinations of negative controls grew on control media (Fig 3a,c) but not on SD-LWH media indicating that AD-PP2AAs combined with BD or AD combined with BD-PP2ACs do not interact (Fig 3b,d). However, slight

transactivation of AD/BD-PP2AC3 was seen but with less growth compared to AD-PP2AA2/BD-PP2AC3 (Fig 3d).

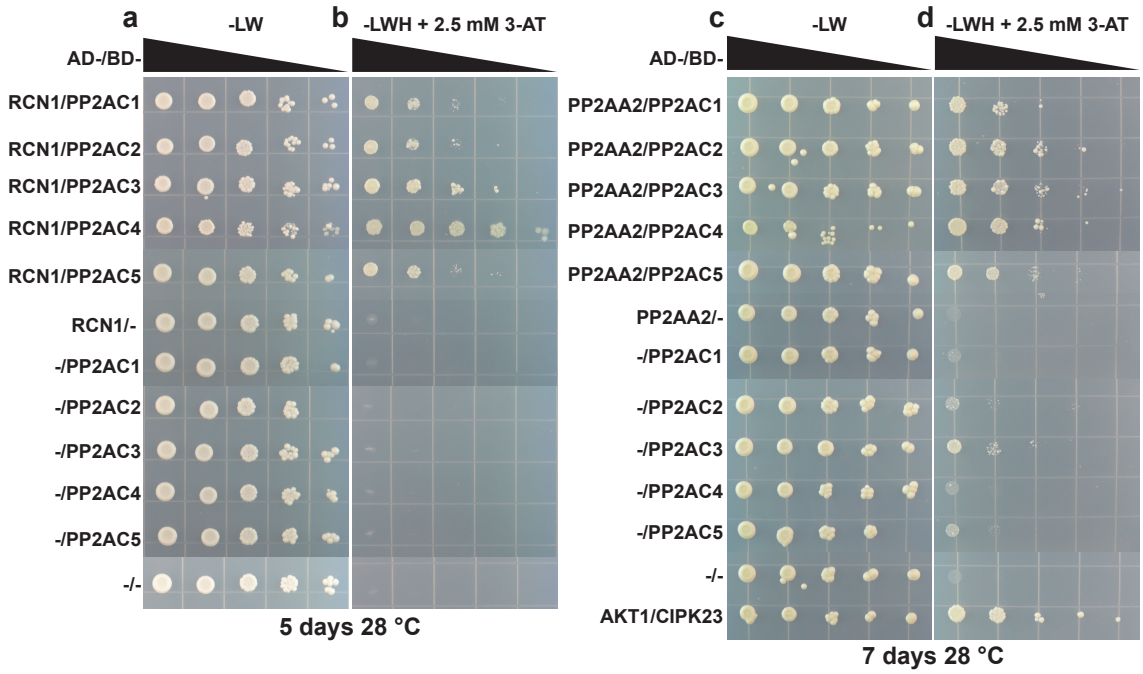

Figure 3. RCN1 and PP2AA2 interact with PP2ACs in Yeast-two-hybrid analyses. Indicated combinations of pGAD.GH-RCN1/PP2AA2 and pGBT9.BS-PP2ACs and empty plasmids were transformed into PJ69-4A. Decreasing ten-fold dilution series ($OD_{600\ nm}$ of 10^{0} - 10^{-4}), indicated by the black arrow, were spotted onto (**b** and **c**), control media (-LW) and (**a** and **c**), selection media (-LWH + 2.5 mM 3-AT) (**b** and **d**), and incubated five-seven days at 28 °C. Yeast growth appeared only when RCN1 and PP2AA2 and PP2ACs were combined and not in combination with empty plasmids. pGAD.GH-AKT1 and pGBT9.BS-CIPK23 interaction (Xu et al., 2006) was used as a positive control.

2.4. PP2As are involved in ABA and stress responses

Previous reports described the role of *rcn1* and *pp2ac2* in ABA responses (Kwak et al., 2002; Pernas et al., 2007). However these analyses used mutants in the Wassilewskija (Ws) background. Here, *pp2a* mutants in the Columbia (Col-0) background were systematically analyzed for ABA responses. Initial analyses of *pp2a* single mutants revealed a role of *rcn1-6, pp2ac3, pp2ac4,* and *pp2ac5* in ABA mediated inhibition of seed germination. These mutants displayed a slight ABA hyposensitivity during seed germination with 1 μM ABA (Fig S2) (assays performed by Rainer Waadt). In contrast to previous reports (Pernas et al., 2007; Ballesteros et al., 2012) the *pp2ac2* mutant allele did not display any ABA mediated seed germination phenotype (Fig S2).

To get further insights into the function of PP2As, seed germination and cotyledon expansion rates were recorded for *pp2a* double mutants without ABA every day for 7 days in 0.5 MS media supplemented $\pm$ 0.5 μM ABA (Fig 4). Starting from day 2 and onward, *rcn1-6/pp2ac3, rcn1-6/pp2ac5,* and *pp2ac3/pp2ac5* (Fig 4j) were found to be ABA hyposensitive, displaying earlier radical emergence and earlier expansion of green cotyledons when compared to Col-0 (Fig 4 e-h,k). In control media without ABA, germination and cotyledon expansion was not affected (Fig a-d,i,k). *rcn1-6/pp2ac3* and *rcn1-6/pp2ac5* exhibited 35% seeds germinated (starting at day 3) compared to 10% in Col-0 as well as 35% cotyledons expanded (measured on day 7) compared to the 10% in Col-0. The data clearly show that on day 3 *pp2ac3/pp2ac5* was the least sensitive to ABA, having 50% seeds germinated compared to the 10% in Col-0 (Fig 4j). *pp2ac3/pp2ac5* also displayed 40% cotyledon expansion compared to the 10% expansion

in Col-0 (Fig 4k). These data indicate that *pp2as* have a negative role in ABA inhibition of seed germination and cotyledon expansion.

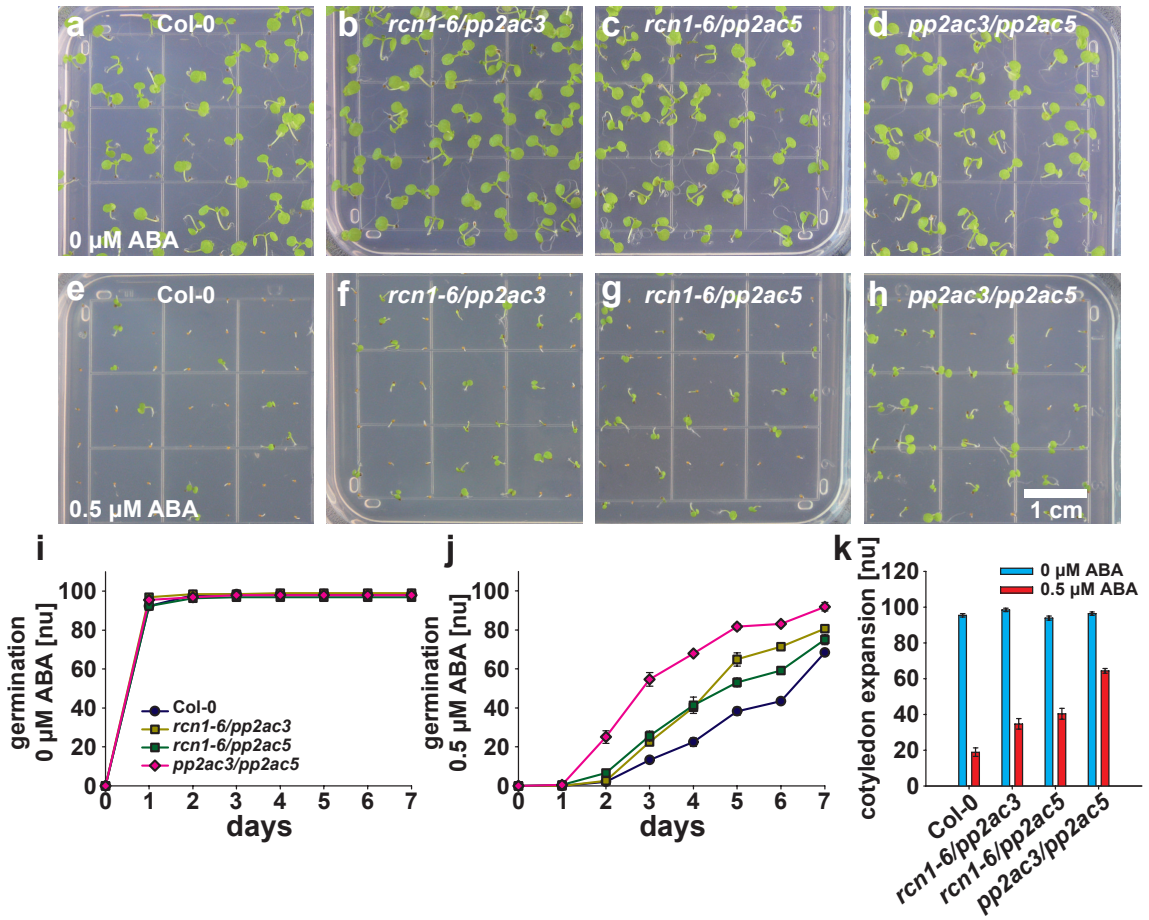

Figure 4. *pp2a* double mutants are ABA hyposensitive in seed germination. Indicated genotypes were grown for seven days in 0.5 MS media (**a-d**), or in 0.5 MS media supplemented with 0.5 mM ABA (**e-h**). Seed germination on media without ABA (**i**) and media supplemented with 0.5 mM ABA (**j**) was recorded for seven days and cotyledon expansion was recorded on the seventh day (**k**). **i-k**, Normalized averages ± s.e.m of four experiments. Compared to Col-0, *rcn1-6/pp2ac3*, *rcn1-6/pp2ac5* and *pp2ac3/pp2ac5* mutants display ABA hyposensitivity in ABA inhibition of seed germination and cotyledon greening/expansion.

Further analyses on *pp2a* mutant seedlings were done to analyze the root growth inhibition by ABA. Previous studies revealed that *pp2ac2* exhibited ABA hypersensitivity during ABA inhibition of root growth (Pernas et al., 2007). Preliminary analyses on single mutants transferred to media with 5 μM ABA displayed an ABA induced root curling phenotype of *rcn1-6* and *pp2ac5* without affecting root length by ABA (Fig S3, assay performed by Rainer Waadt). The *pp2ac2* single mutant did not display any enhanced root growth inhibition (Fig S3). Analyses of double mutants revealed that even in 0.5 MS control conditions the root growth of *rcn1-6/pp2ac2*, *rcn1-6/pp2ac3,* and *rcn1-6/pp2ac5* was affected (Fig 5a,c). *rcn1-6/pp2ac3* and *rcn1-6/pp2ac5* displayed shorter roots even in ABA free 0.5 MS media (Fig 5c). Application of 5 μM ABA resulted in an additive effect, where a strong decrease in root length compared to Col-0 wild type was observed (Fig 5b-f). Strong root growth inhibition at 5 μM ABA was found for *rcn1-6/pp2ac2* (Fig 5b), *rcn1-6/pp2ac5* (Fig 5d), *pp2ac3/pp2ac5* and *pp2ac4/pp2ac5* (Fig 5f), with *pp2ac3/pp2ac5* exhibiting the strongest inhibition of root growth (Fig 5b,d,f,g). Root growth of Col-0 was inhibited by ABA to 85% of control conditions while *rcn1-6/pp2ac2, pp2ac3/pp2ac5, pp2ac4/pp2ac5* displayed 45% root length of the control conditions and *rcn1-6/pp2ac5* displayed 70% root length (Fig 5g). Root length of *rcn1-6/pp2ac3* was not affected by ABA (Fig 5g), however stronger root curling was observed in presence of ABA (Fig 5d). Interestingly, the ABA seedling growth assay displayed a hypersensitive ABA phenotype (Fig 5) while the seed germination assay displayed a hyposensitive phenotype (Fig 4).

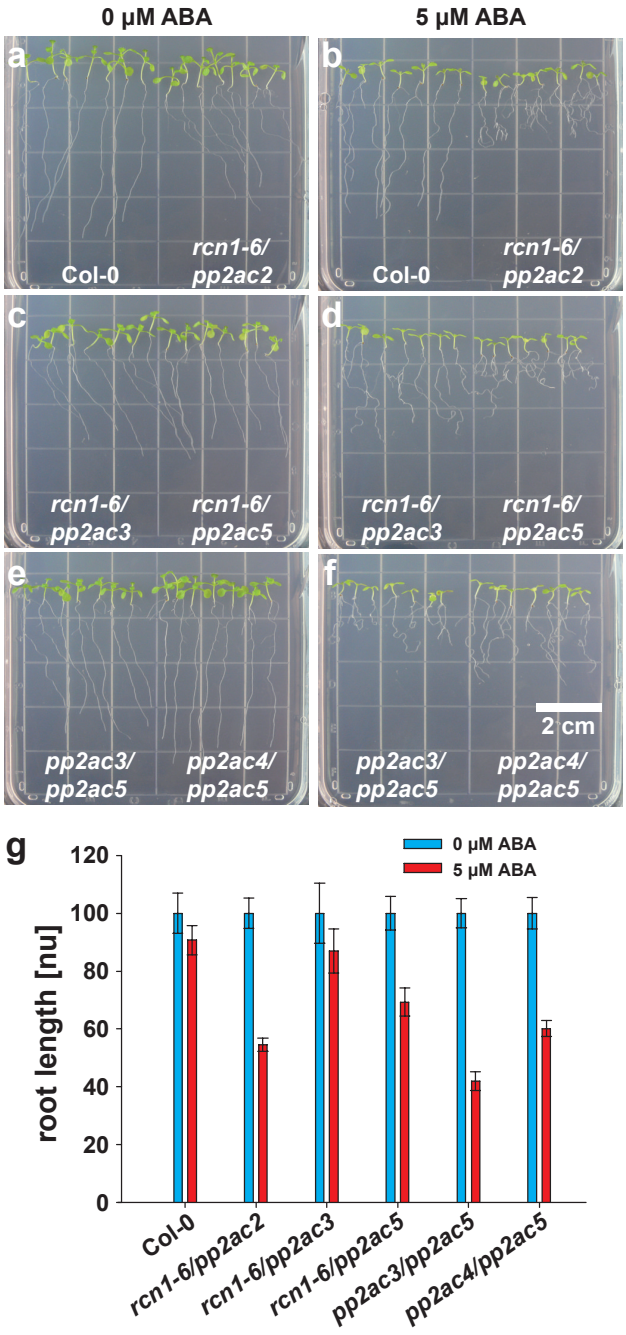

Figure 5. Roots of *pp2a* double mutants are hypersensitive to ABA. a-f, Four-day-old seedlings of indicated genotypes were transferred to 0.5 MS media without (**a**, **c**, **e**) or with 5 µM ABA (**b**, **d**, **f**) and grown for additional five days before images were acquired. **g**, Root length of indicated genotypes five days after transfer to 0.5 MS media ± 5 µM ABA was normalized to the root length in control conditions (0.5 MS + 0 µM ABA). Data represent averages +/- s.e.m. of five experiments. Compared to Col-0, *rcn1-6/pp2ac2*, *rcn1-6/pp2ac5*, *pp2ac3/pp2ac5* and *pp2ac4/pp2ac5* exhibit a strong inhibition of root growth in the presence of 5 µM ABA.

It is well known that ABA plays essential roles in the regulation of stomatal movements (Kim et al., 2010). RCN1 was identified from guard cell cDNA libraries and the *rcn1* mutant in Wassilewskija ecotype (Ws) displayed an ABA-insensitive stomatal response (Kwak et al., 2002). Thus, it was of interest to analyze stomatal movements with *rcn1-6* and *pp2ac* double mutants in Col-0 ecotype. Detached leaves were incubated 2h in opening buffer (pH 6.15) before stomatal closure was induced by 5 μM ABA. Despite the *rcn1* phenotype in Ws background, none of the Col-0 background double mutants investigated (*rcn1-6/pp2ac2, rcn1-6/pp2ac3, rcn1-6/pp2ac5, pp2ac3/pp2ac5,* and *pp2ac4/pp2ac5*) exhibited altered ABA responses compared to Col-0 wild type 2h after ABA treatment (Fig 6). All of the investigated lines closed their stomata to 80% of the stomatal aperture in control conditions (Fig S6).

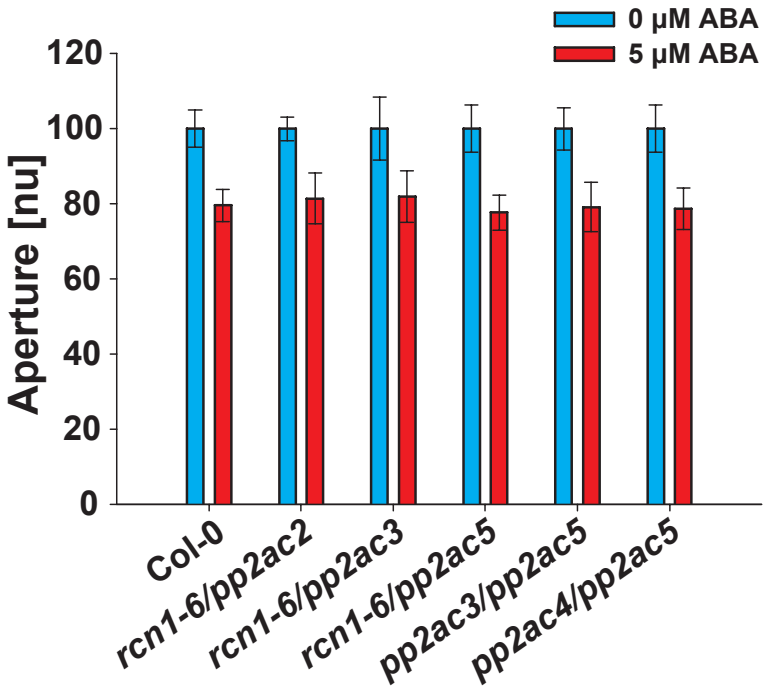

Figure 6. ABA-induced stomatal closure is not altered in *pp2a* double mutants.
Detached leaves of indicated genotypes were incubated in opening buffer for two hours and subsequently EtOH, as solvent control, (0 µM ABA) or 5 µM ABA was added followed by additional two hours incubation. Images of 20 stomata were acquired after enrichment using the blending method. Data represent stomatal aperture averages ± s.e.m. of four experiments normalized to the 0 µM ABA control. The investigated *pp2a* double mutants display ABA induced stomatal closure similar to Col-0.

rcn1 mutant seedlings displayed abnormalities in ionic stress conditions at the root apical meristem, connecting their role to stress signaling (Blakeslee et al., 2008). A salt-stress assay was performed to analyze the effects of 100 mM NaCl on roots of *pp2a* single and *ost1-3* mutant seedlings (Fig S4). Four-day-old seedlings were transferred to 0.5 MS media supplemented $\pm$ 100 mM NaCl (Fig S4a-h) and root lengths (Fig S4i) and fresh weight (Fig S4j) were measured five days after transfer. *rcn1-6* and *pp2ac5* exhibited increased sensitivity to NaCl stress with a strong decrease in root growth (50% of control conditions) compared to Col-0 wild type (80% of control conditions) (Fig S4f,h,i). The other *pp2a* single mutants and *ost1-3* appeared similar to wild type (Fig S4). In addition, the salt-induced fresh weight loss was slightly enhanced in *rcn1-6*, *pp2aa3, pp2ac3, pp2ac4,* and *pp2ac5* but not in *ost1-3* and *pp2ac2* when compared to wild type Col-0 (Fig S4j).

To investigate if PP2AC overexpression could rescue *pp2a* mutant phenotypes PP2AC3-, PP2AC4-, and PP2AC5-mVenus constructs were expressed under control of the pUBQ10 promoter (Norris et al., 1993; Krebs et al., 2011) in the respective *pp2ac* mutant background. Surprisingly it was found that strong expressing lines for all PP2ACs analyzed exhibited severe dwarfism and reduced growth phenotype (Fig S5 b-d, e-f right) when compared to Col-0 (Fig S5a, e-f left). These phenotypes were similar to brassinosteroid synthesis or signaling mutants (Li and Chory, 1997; Tang et al., 2011) indicating that PP2AC-mVenus constructs might act dominant negative through masking of the regulatory C-terminus by the mVenus fusion. Lines with strong phenotype did not produce seeds and could not be analyzed in following generations. Only lines with

weaker phenotypes could be analyzed in following generations, however no homozygous lines could be identified.

2.5. PP2As and OST1 interact in BiFC and Co-IP analyses

To get further insights into the involvement of PP2As in the ABA signaling pathway, protein-protein-interaction analyses were performed with PP2As and OST1. OST1 has been identified as a key component of ABA signal transduction (Mustilli et al., 2002; Merlot et al., 2002; Yoshida et al., 2002). BiFC analyses of OST1 and all three PP2AAs, PP2AB'alpha, PP2AB'beta, and PP2AB'delta, and of all five PP2ACs were analyzed and compared to the OST1-ABI1 interaction (Yoshida et al., 2006; Umezawa et al., 2009) used as a positive control (Fig 7). For this assay, OST1 was fused to the N-terminal fragment of YFP (YN-OST1) and co-expressed in *N. benthamiana* epidermal cells with PP2As or ABI1 fused to C-terminal fragment of YFP (YC-PP2As and YC-ABI1). In microscopic analyses YN-OST1 and YC-ABI1 displayed high YFP fluorescence and the OST1-ABl1 complex localized in the nucleus and the cytoplasm (Fig 7l). Also, interaction of YN-OST1 with all three YC-PP2AAs resulted in an unexpected strong reconstitution of YFP fluorescence, showing complex formations in the nucleus and the cytoplasm (Fig 7a-c,m). Interestingly, the highest YFP fluorescence, among OST1-PP2A interactions, was observed between YN-OST1 and YC-PP2AA3 (Fig 7m). Interaction was also observed between YN-OST1 and YC-PP2AB'alpha, -B'beta, and –B'delta, though not as strong when compared to PP2AAs (Fig 7m). OST1 interaction with PP2AB'alpha and PP2AB'beta was found in the cytoplasm, the nucleus, and in dot-like structures, while the interaction of OST1 with PP2AB'delta was restricted from the nucleus (Fig 7d-f). YFP fluorescence of YN-OST1 YC-PP2ACs complexes was insignificant compared to combinations of PP2AAs and PP2ABs (Fig 7m), but

complexes were localized in the cytoplasm, the nucleus and in dot like structures (Fig 7g-k) similar to interactions with PP2AB'alpha and PP2AB'beta (Fig 7d,e).

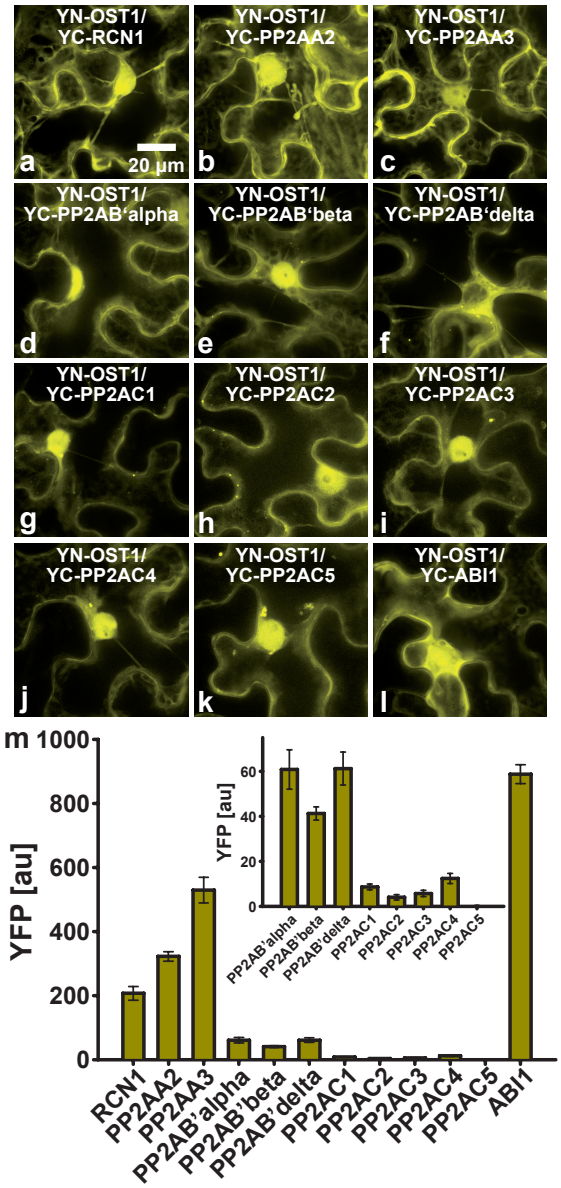

Figure 7. PP2As interact with OST1 in BiFC analyses. OST1 was fused to the YFP N-terminal fragment (YN-OST1) and PP2As and ABI1were fused to the YFP C-terminal fragment (YC-PP2A; YC-ABI1) and indicated construct combinations were co-expressed in *N. benthamiana*. Images were acquired three to four days after transformation. **a-l**, Maximum projections of 32-z-stack-images showing the sub-cellular localizations of indicated OST1-PP2A and OST1-ABI1 complexes. **m**, Semi-quantitative analyses of reconstituted YFP emission of indicated OST1-PP2A and OST1-ABI1 BiFC combinations were compared to OST1-ABI1 interaction. For better comparison of the emission signals the scale in the inset was adjusted. OST1 interacts strongest with ABI1 and PP2AAs in the cytoplasm and the nucleus. Interaction of OST1 with PP2ABs and PP2ACs was found in the cytoplasm, nucleus and in dot-like-structures, except of interaction with PP2AB'delta, which was absent from the nucleus.

To further validate OST1 interaction with PP2AAs, interaction of OST1 with all three PP2AAs and with PP2AB'alpha, -B'beta, and -B'delta and PP2AC3 was analyzed in *in vivo* Co-IP experiments (Fig 8). OST1 was fused with 6xHis-3xFLAG-tag at its C-terminus (OST1-HF) while PP2AAs and PP2ABs were fused to m-Turquoise tag at their N-terminus and PP2AC3 to an mVenus tag at its N-termuns (mT-PP2As, mVenus-PP2AC3; see also Fig 1a-c and Fig 1g-i,o) and expressed in *N. benthamiana*. OST1-HF co-expressed with mTurquoise alone was used as a negative control. The Co-IPs were performed using anti-FLAG magnetic beads to purify OST1-HF. After western blotting, OST1-HF was detected by anti-FLAG (Fig 8a,c) and mT-PP2As by anti-GFP antibodies (Fig 8b,d). All mT-fusion proteins were detected after protein extraction (Fig 8b,d input lanes). Specific interactions (IP lanes) were found between OST1-HF and mT-RCN1 and mT-PP2AA3 (Fig 8a,b). However, mT-PP2AA2 and mT alone could not be detected in western analyses after OST1-HF purification. It also appeared that OST1-PP2AA3 interaction was strongest (Fig 8b), consistent with BiFC analyses (Fig 7m). Additional Co-IP experiments confirmed the interaction of OST1 with PP2AB'alpha, PP2AB'beta and PP2AB'delta (Fig 8c,d). However, interaction of OST1 with PP2AC3 was only marginal when compared to interactions with PP2ABs (Fig 8d), which was also consistent with BiFC analyses (Fig 7m).

These results strongly demonstrate the physical interaction of OST1 with PP2As, however the functional consequence of these interactions still needs to be determined. Preliminary mass spectrometric analyses after co-purification of OST1-HF and mT-PP2AB'beta suggested phosphorylation of PP2AB'beta at S14 and/or S16. It was found that homologous Ser residues in other PP2AB'-subunits are conserved and that S14

homologous residues for example in PP2AB'gamma, PP2AB'zeta, and in PP2AB'kappa perfectly match the OST1 consensus target site (Fig 8e) (Sirichandra et al., 2010).

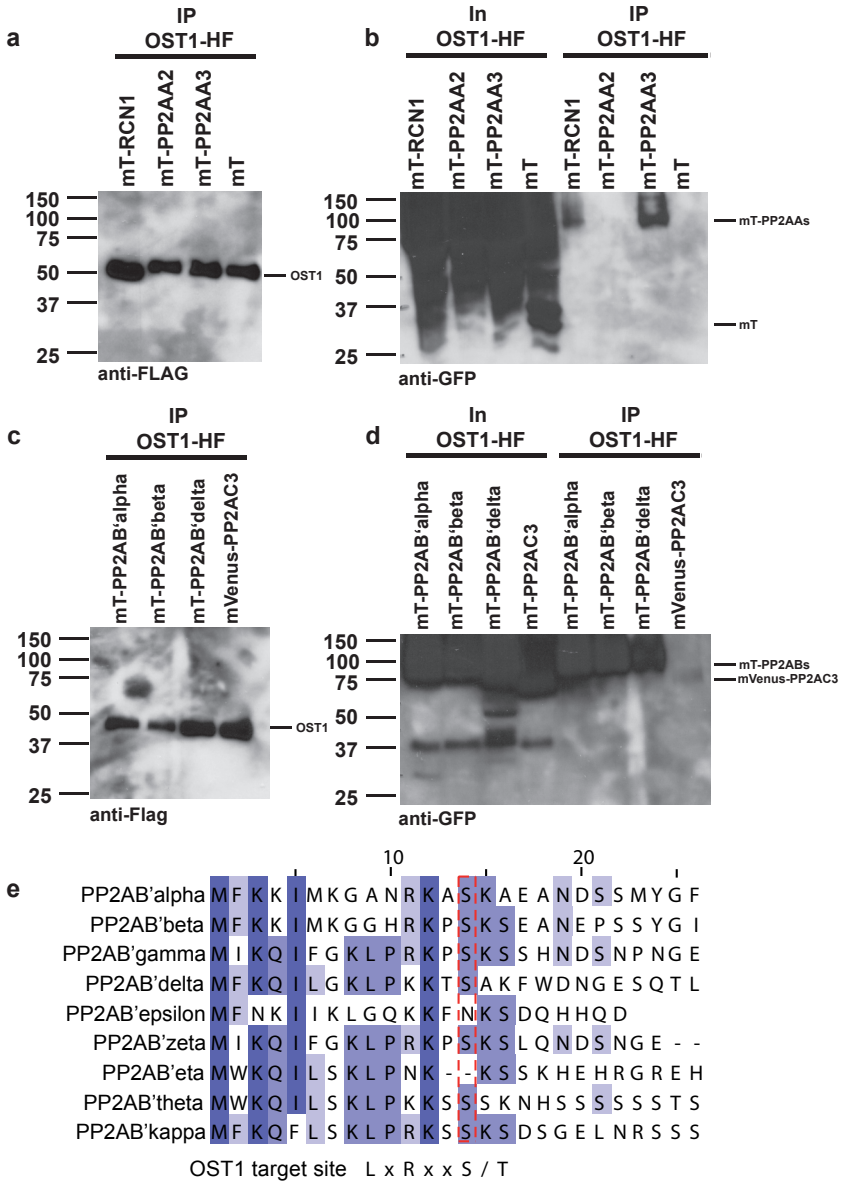

Figure 8. Co-IP experiments of PP2A interaction with OST1. Co-IP experiments were performed with OST1-HF (6xHis3xFLAG) against mTurquoise-(mT)-RCN1, PP2AA2, PP2AA3 subunits and mT alone as negative control (**a**,**b**) mT-PP2AB'alpha, -'beta, -'delta and mVenus-PP2AC3 (**c**,**d**). Constructs were infiltrated into *N. benthamiana*. Three days later, *N. benthamiana* leaves were activated for one hour by osmotic stress and OST1-HF proteins were co-purified using anti-FLAG magnetic beads (**a**,**c**). Immunoblotting, using an anti-GFP antibody, was used to detect co-purification of mT-(PP2As) (**b**,**d**). Input (In) lanes display protein extracts; IP lanes display samples after purification. **c)** MuscleWS alignment of the PP2AB' N-termini, colored by percentage identity in JalView2.8 (Waterhose et al., 2009). S14 of PP2AB'beta and homologous residues are framed in the red box. The OST1 target site (Sirichandra et al., 2010) is indicated below the alignment.

Taken together, it was found that *pp2a* double mutants display reduced ABA sensitivity during seed germination and enhanced ABA sensitivity in the root. These ABA related phenotypes could be linked to physical interaction with OST1, which might potentially phosphorylate PP2AB subunits.

3. DISCUSSION

3.1 Subcellular localization and physical interaction of PP2A-subunits

Type 2A protein phosphatases are involved in many aspects of plant hormone biosynthesis, transport, and signal transduction (summarized in the introduction). However, the subcellular localizations and functions of specific PP2AAs and PP2ACs have not been analyzed so far in depth. To analyze the localization patterns of the different PP2As, fluorescent protein fusions of PP2As were expressed in *N. benthamiana* leaf epidermal cells. For all PP2AAs, mTurquoise-PP2AA and PP2AA-mVenus fusion proteins were localized in the nucleus and in cytoplasmic strains (Fig 1a-f). The nuclear and cytoplasmic localization was consistent with previous studies on RCN1 and PP2AA3 subcellular localization (Blakeslee et al., 2008; Terol et al., 2007).

The PP2AC C-terminal TPDYFL tail is highly conserved and methylation of the last L residue is important for PP2A activity and holoenzyme assembly (Sents et al., 2012). Recently, a methyltransferase SBI1 was identified in a forward genetic screen as *suppesor for bri1* (Wu et al., 2011). The function of this methyltransferase was linked to methylation of the PP2AC C-terminal tail, supporting the importance of PP2AC methylation in brassinosteroid signaling. One potential PP2AC subunit, which mediates brassinosteroid responses, is PP2AC5. The *pp2ac5* mutant displayed shorter hypocotyl elongation when grown in the dark (Rainer Waadt unpublished data) and also on media supplemented with brassinazole (Tang et al., 2011). Overexpression of PP2ACs where the C-terminal Leu-tail was masked by an mVenus fusion tag displayed strong dwarfism and sterility (Fig S5), similar to brassinosteroid synthesis and signaling mutants (Li and Chory 1997, Tang et al., 2011). These data support that suppression of the PP2AC Leu-tail and overexpression of such constructs might lead to dominant negative effects of

PP2As. Potentially these PP2AC-mVenus fusions are not active and inhibit PP2A activity when incorporated into the PP2A holoenzyme complex. For the subcellular localization of PP2ACs, only mVenus-PP2ACs were analyzed. mVenus-PP2AC fusion proteins were localized in the nucleus and in cytoplasmic strains but also in dot-like structures (Fig 1m-q).

The PP2ABs were more differentially distributed in the cell. Upon expression in *N. benthamiana*, the PP2ABs seemed to have a necrotic effect on the tobacco leaves. Therefore PP2AB'alpha, PP2AB'epsilon, and PP2AB'eta were expressed under control of an inducible β-estradiol promoter, which reduced toxic effects (Schlücking et al., 2013). Both fusion proteins of PP2AB'alpha and PP2AB'beta were found in the nucleus and in cytoplasmic strains, with stronger signal in the nucleus (Fig 1g,h,j,k). mTurquoise-PP2AB'delta was found in cytoplasmic strains (Fig 1j) while PP2AB'delta-mVenus was found in dot-like structures and the plasma membrane (Fig 1l). PP2ABalpha and PP2AB'gamma were identified in the cytoplasm (Fig S1a,b,f,g). While mT-PP2AB'epsilon localized in the cytoplasm and the nucleus (Fig S1c), PP2AB'epsilon-mVenus was found in microdomains of the plasma membrane (Fig S1h). PP2AB'zeta, PP2AB'eta, and PP2Ab'theta fluorescent protein fusions were localized in the nucleus, nucleolus, and in dot-like structures (Fig S1i-k and Fig S1d,e). PP2AB'eta-mVenus exhibited also strong fluorescence at the plasma membrane (Fig S1j). Data in Fig S1 in part confirmed previous sub-cellular localization analyses of PP2AB'gamma, PP2AB'zeta, PP2AB'eta, and PP2AB'theta (Matre et al., 2009). In these studies PP2AB'gamma localized in the nucleus and cytosol, PP2AB'zeta was found in the cytoplasm and in mitochondria, PP2AB'eta was identified in the nucleus, nucleolus and

the cytoplasm, while PP2AB'theta was found in the cytoplasm, nucleus, and peroxisomes (Matre et al., 2009). However, differences in subcellular localizations using mT fused to the PP2AB N-terminus or mVenus fused to the PP2AB C-terminus, toxic effects, and low expression of PP2ABs in *N. benthamiana* make it difficult to conclude about the exact localization of certain PP2AB subunits. Similar to localization analyses of PP2ABs (Matre et al., 2009), the results revealed that the different PP2AB-isoforms target different compartments of the cell, supporting the hypothesis that PP2AB-subunits are necessary for the subcellular localization of the PP2A holoenzyme in plants (DeLong, 2006; Farkas et al., 2007). Because there are over 255 possible holoenzyme combinations (due to the high number of PP2ABs), it is important to analyze interactions between PP2A subunits to determine if there is complex specificity for PP2A subunit combinations.

Experimental evidence of physical interactions of PP2As has not yet been reported *in planta* (Ballesteros et al., 2012). To study these interactions *in vivo*, BiFC and yeast-two-hybrid analyses were performed. BiFC experiments revealed interactions between all PP2AAs and PP2ACs, with RCN1 (PP2AA1) and PP2ACs displaying the strongest reconstitution of YFP fluorescence (Fig 2p). Yeast-two-hybrid analyses were performed to confirm the physical interactions of RCN1 and PP2AA2 with PP2ACs (Fig 3). Results were consistent, displaying that both RCN1 and PP2AA2 can interact with all five PP2ACs (Fig 3b,d). However, strongest interaction was found between RCN1 and PP2ACs, more specific with PP2AC4, in both experiments (Fig 2p and Fig 3b). These findings support that RCN1 is the preferred interaction partner of PP2ACs, and that the other two PP2AAs do not have equivalent effects on overall PP2A activity when RCN1 is

functional (Blakeslee et al., 2008). All PP2AAs can interact with all PP2ACs (Fig 2 and Fig 3), however with different interaction intensities. It appears that there is no strong evidence for complex specificity for PP2AA and PP2AC interactions. Further interaction experiments should be performed to determine if there is complex and subcellular localization specificity between PP2AAs and PP2ABs and if PP2ABs and PP2ACs can interact in absence of PP2AAs.

3.2 Functional roles of PP2As in ABA responses

Analyses of *pp2a* mutants have revealed that regulatory PP2AA and catalytic PP2AC subunits are components of the ABA signaling pathway (Kwak et al., 2002; Pernas et al., 2007). ABA plays an important physiological role in plants. It inhibits seed germination and promotes seed dormancy (Finkelstein et al., 2008), inhibits root growth and lateral root formation (De Smet et al., 2006; Duan et al., 2013), and promotes stomatal closure (Schroeder et al., 2001; Kim et al., 2010). Here the involvement of PP2AA and PP2AC single and double mutant combinations in ABA responses during germination, root growth and stomatal closure were analyzed.

Preliminary data indicated that the loss of function mutants *rcn1-6, pp2ac3, pp2ac4,* and *pp2ac5* conferred a slightly hyposensitive response to ABA in seed germination (Fig S2). The analysis of the double mutants displayed an additive phenotypic effect when double mutant combinations of *rcn1-6, pp2ac3,* and *pp2ac5* were analyzed. In these analyses, *pp2ac3/pp2ac5* displayed the least ABA sensitivity in seed germination and cotyledon expansion (Fig 4j). *pp2ac2* in Ws background was found to be ABA hypersensitive (Pernas et al., 2007). Interestingly, *pp2ac2* in Col-0 exhibited no

phenotype in ABA seed germination experiments (Fig S2k,q). A reason for the *pp2a* ABA hyposensitivity in seed germination could be due to a cross talk between ABA and ethylene. Ethylene plays many important roles in plants including the promotion of seed germination (Abeles et al., 1992). *rcn1 (eer1)* was recently found in a forward genetics screen for enhanced ethylene response (Larsen and Cancel, 2003) and it was shown that *RCN1* regulates the turnover of ethylene biosynthesis genes (Skottke et al., 2011). Treatment of wild type seedlings with PP2A inhibitors resulted in increased ethylene response (Larsen and Cancel, 2003). This could be one explanation why the *pp2a* double mutant combinations were less sensitive to ABA in germination (Fig 4), probably due to enhanced ethylene levels during seed germination.

PP2A mutants were also analyzed for ABA mediated inhibition of root growth. Interestingly, preliminary data displayed *rcn1-6* and *pp2ac5* to have a hypersensitive response to ABA in root growth/curling (Fig S3), which differed to the hyposensitive response to ABA in seed germination. However, similar to seed germination assays, the analysis of *pp2a* double mutants displayed an additive phenotypic effect in presence of 5 μM ABA (Fig 5 b,d,f). *rcn1-6/pp2ac2, pp2ac3/pp2ac5,* and *pp2ac4/pp2ac5* exhibited strong ABA mediated inhibition of root growth with enhanced root curling (Fig 5g). *rcn1* was identified in a forward genetics screen for root curl in NPA (Gabers et al., 1996) and root curling phenotypes were also observed for *rcn1-6* (Blakeslee et al., 2008). NPA is an inhibitor of auxin transport and it has been reported that *pp2aa* subunit mutations affect the polarity of PIN auxin transporters (Michniewicz et al., 2007). The enhanced root curling of *pp2as* in ABA, support that PP2As are involved in ABA and auxin crosstalk during root development and stress responses. *PP2AC3* and *PP2AC4,* which are involved

in plant patterning through their function in establishing auxin gradients, (Ballesteros et al., 2012) are possible candidates for functions in ABA and auxin crosstalk.

rcn1 mutant seedlings also displayed abnormalities in ionic stress conditions at the root apical meristem, connecting their role to stress signaling (Blakeslee et al., 2006). A salt-stress assay with 100 mM NaCl was performed to analyze the effects of salt on root growth of single *pp2a* mutant seedlings and of *ost1-3* (Fig S4)**.** *rcn1-6* and *pp2ac5* exhibited increased sensitivity to NaCl stress with a strong decrease in root elongation compared to Col-0 wild type (Fig S4i). Fresh weight of *pp2a* single mutants was also slightly affected by 100 mM NaCl (Fig S4j). However, the salt sensitivity if *pp2ac2* (Pernas et al., 2007) was not observed in these analyses (Fig S4g,i).

During seed germination PP2As might mediate ABA and ethylene crosstalk, while in the root a crosstalk between ABA and auxin is perceived by PP2As. For example, the ABA inhibition of lateral root formation in ionic stress conditions (Duan et al., 2013) might be transmitted through *RCN1* and *PP2AC5* (Fig S3) or other *RCN1-PP2AC* complexes (Fig 5g). However, involvement of PP2As in different hormone signaling pathways make it difficult to analyze the opposing phenotypes in seed germination and root growth.

Different combinations of PP2As form complexes with unique properties, which in animals are known to regulate a range of developmental processes (Janssens and Goris, 2001). Thus, it is surprising that a disruption in one single gene can result in a strong observable phenotype. In the ecotype Wassilewskija, *rcn1* displayed an ABA and MeJA insensitive phenotype in guard cells (Kwak et al., 2002; Saito et al., 2008). However, in preliminary analyses of *rcn1-6* in Col-0 background, no guard cell phenotype was

observed (data not shown). Also none of the investigated mutant combinations of *rcn1-6* and *pp2ac2, pp2ac3,* and *pp2ac5* displayed any ABA-induced stomatal closure phenotype (Fig 6). The guard cell phenotype of Ws *rcn1* might be an ecotype specific response or it could mean that the ABA response in guard cells, which is mediated through PP2As is more robust in Col-0. Potentially multiple PP2A holoenzyme combinations could function in the ABA-induced stomatal closure response. *RCN1* has also been found to interact with and down-regulate the blue light-activated *PHOT2* (blue light receptor) (Tseng and Briggs, 2010). Also, *PP2AC2* plays a functional role in modulating blue-light induced chloroplast movements by regulating actin skeleton in plants (Wen et al., 2012). *PP2A* and *PHOT2* interaction could be a link between the ABA and blue light signaling pathways in guard cells, however the PP2A subunits involved in this processes in Col-0 still need to be identified.

Thus far, the *pp2a* mutants with the strongest ABA phenotypes are double mutant combinations of *rcn1-6* and *pp2ac5* (Fig 4 and Fig 5). The involvement of PP2As in ABA signaling leads to the question about the molecular mechanism of these responses. Because PP2As play important roles not only in ABA but also in other hormone signaling pathways including auxin, brassinosteroid, ethylene, MeJA, and blue light, PP2As could be the hub in the cross talk between different signaling pathways.

3.3 Physical interactions of PP2As with OST1

To determine potential PP2A interactors, which are involved in ABA signaling, BiFC experiments were performed with OST1 (Fig 7). OST1 encodes for an ABA-

activated protein kinase, a member of SNF1-related protein kinases (SnRK2) (Yoshida et al., 2002; Boudsocq et al., 2004). It has been identified as a key component of ABA signal transduction in guard cells (Mustili et al., 2002; Merlot et al., 2002; Yoshida et al., 2002), making it an excellent candidate as an interactor with PP2As. OST1 is known to interact with another class of phosphatases, namely PP2Cs (Yoshida et al., 2006; Umezawa et al., 2009), which are directly targeted and inhibited by PYR/PYL ABA receptors (Ma et al., 2009; Park et al., 2009; Santiago et al., 2009). To analyze and compare the interaction strengths of PP2AAs, PP2ABs, and PP2ACs with OST1, OST1-ABI1 interaction was used as a positive control (Fig 7l) (Yoshida et al., 2006; Umezawa et al., 2009). In BiFC experiments all three PP2AAs interacted strongly with OST1 in the nucleus and the cytoplasm, while the strongest reconstitution of YFP fluorescence was unexpectedly seen with PP2AA3 and not with RCN1 (Fig 7m). An ABA related phenotype *pp2aa3* has not been identified so far (Fig S2 and Fig S3). BiFC results also displayed interaction of OST1 and PP2AB'alpha, PP2AB'beta, and PP2AB'delta in the nucleus and cytoplasm, with OST1-PP2AB'delta complexes excluded from the nucleus (Fig 7d-f). However, weaker YFP fluorescence was observed in comparison to PP2AAs (Fig 7m). The PP2ACs displayed very weak YFP fluorescent reconstitution, which may be due to complex localization in "dot-like structures," (making the small localization area difficult to quantify YFP fluorescence). Unfortunately, the interactions of OST1 and the PP2As analyzed in the BiFC experiments could not be confirmed in yeast-two hybrid assays (data not shown). Interactions might be too transient in yeast or plant components for the interaction are missing in yeast (e.g. OST1 might interact only with the PP2A holoenzyme or needs itself a scaffolding protein to interact with PP2As).

An *in-vivo* Co-IP assay was performed with OST1 against the three PP2AAs and three PP2ABs, to confirm the BiFC results (Fig 8). Immunoblots demonstrated the strong interaction of OST1 with PP2AA3 (Fig 8b) and interaction with RCN1 (Fig 8b), PP2AB'alpha, PP2AB'beta, and PP2AB'delta (Fig 8d). Because OST1 interacted with all three PP2ABs in the Co-IP experiments, it would also be interesting to see if OST1 interacts with other PP2ABs. Data, supporting RCN1 in being the key PP2AA subunit in regulation of PP2A activity (Zhou et al., 2004; Michniewicz et al., 2007) and the preferred interaction partner with PP2ACs and PP2ABs (Blakeslee et al., 2008) makes it valid to hypothesize that RCN1 would exhibit the strongest functional interaction with OST1. In addition, PP2AA3 had no ABA root and germination phenotypes (Fig S2 and S3). However, the strong PP2AA3-OST1 interaction in BiFC and *in-vivo* Co-IP experiments indicate there could be holoenzyme formation specificity that favors regulatory PP2AA3 in regards to OST1 interaction. This, along with the similar expression levels of *RCN1* and *PP2AA3* in guard cells (EFP browser Winter et al., 2007), could explain the lack of stomatal phenotypes of *rcn1-6* and the investigated *pp2a* double mutants (Fig 6). Because PP2AA3-OST1 interaction is the strongest, *pp2aa3/pp2ac* or *rcn1-6/pp2aa3* double mutant combinations could reveal the stomatal phenotype. This then leads to the question if the PP2AAs and PP2ABs interact with SnRK2s in general, specifically with the other ABA-activated SnRK2.2 and SnRK2.3 (Boudsocq et al., 2004). These SnRK2s are important in ABA signaling in roots and seed germination (Fujii et al., 2007). If PP2As interact with SnRK2s other than OST1, it may also explain the root and germination phenotype of *pp2as,* as OST1 is predominantly expressed in guard cells (EFP browser Winter et al., 2007). PP2AB'beta S14 or S16 were identified in

mass spectrometric analyses to be phosphorylated after Co-IP with OST1. S14 in PP2AB'beta and homologous sites in other PP2AB'-subunits match the OST1 target phosphorylation site LxRxxS/T (Srichandra et al., 2010; Fig 8c). The current hypothesis is that OST1 potentially phosphorylates PP2AB' subunits. However, the functional consequence of such a phosphorylation still needs to be determined. Interestingly, the PP2AB'-subunits found to interact with OST1 also strongly interact with BZR1, the core transcription factor in the brassinosteroid signaling pathway (Tang et al., 2011). This might be a link to ABA and brassinosteroid crosstalk. In future work, the aim would be to identify also potential phosphorylation sites in PP2AAs. In gel kinase assays of ABA activated SnRK2s in *pp2a* mutants could indicate if *pp2as* are involved in the regulation of SnRK2 activity. *Vice versa* phosphorylation assays could determine if PP2As are substrates of OST1 *in vitro*. Finally *pp2a* activity assays in *ost1-3* and *snrk2/3* in presence and absence of ABA could give an indication about activation or inhibition of PP2As by SnRK2s, which could be integrated into the crosstalk mechanisms of ABA with other plant hormones.

4. MATERIALS AND METHODS

4.1. T-DNA, overexpression-lines and genotyping

T-DNA lines were obtained from Arabidopsis Biological Resource Center and from Nottingham Arabidopsis Stock Centre. The *rcn1-6* allele was kindly provided by Dr. Alison DeLong (Brown University). T-DNA insertions were confirmed by PCR on genomic DNA and sequencing of the left- and right-borders. Genomic DNA was isolated using the CTAB method. RNA was isolated using RNeasy Plant Mini Kit (Quiagen) and reverse transcribed using the First-Strand cDNA Synthesis Kit and Not I $d(T)_{18}$ primers (GE Healthcare). Mutant status was confirmed by RT-PCR (38 cycles) including actin2 primers for expression control. A detailed list of primers is provided in Table S1. Genomic maps of PP2As including details about T-DNA lines and RT-PCRs results are provided in Figure S6 and Figure S7. RT-PCR results of *pp2a* double mutants are provided in Fig S8.

Coding sequences of PP2ACs were cloned with an mVenus-tag at their C-terminus into pGBTVII bar vector harboring the pUBQ10 and HSP18.2T and transformed into the respective *pp2ac* T-DNA line by the floral dip method (Clough and Bent, 1998). Positive transformants were selected on 0.5 MS media supplemented with 10 μg/L glucosinate and by microscopic analyses of mVenus fluorescence. Positive transformants which could produce seeds were further propagated and analyzed.

4.2. Plant growth and phenotypical analyses

Arabidopsis seeds were surface sterilized in 70 % EtOH and 0.04 % SDS followed by three washes in 100 % EtOH and sowed on 0.5 MS media (Sigma) (pH 5.8) supplemented with 0.8 % Phyto Agar (RPI). After four days of stratification at 4°C in the

dark plants were grown in a growth room in long day conditions (16 h light/8 h dark) with 50 - 80 mE m^{-2} s^{-1} light intensity at 27 °C. Six day old seedlings were transferred to pots for further growth. For stomatal bioassays plants were cultivated in a Conviron CMP3244 plant growth chamber with 16 h day, 22 °C/8 h night, 18 °C cycle and 50-100 mE $m^{-2}s^{-1}$.

For ABA seed germination assays seeds were sown on 0.5 MS agar plates supplemented ± 0.5 µM (+)-ABA (TCI) or 1 µM (+/-)-ABA (Sigma). After four days of stratification seed germination (radicle emergence) and cotyledon expansion were recorded for a time period of 7 days with blinded genotypes. Analyses represent % germination (average ± s.e.m.) of four technical replicates.

For root growth assays, seven four-day-old seedlings were transferred to 0.5 MS agar plates supplemented with ± 5 µM ABA or 100 mM NaCl and grown vertically in the growth room. Images were acquired five days after seedling transfer and root length was analyzed using Fiji (http://fiji.sc/Fiji; Schindelin et al., 2012) or the Root Detection software (http://www.labutils.de/rd.html). Root length and fresh weight were analyzed as averages of seven seedlings ± s.e.m of 5 technical replicates and normalized to the data of the 0.5 MS control conditions.

ABA-induced stomatal closure analyses were performed with detached leaves of four-week-old plants, which were floated in stomatal bioassay buffer (5 mM KCl, 50 µM $CaCl_2$ and 10 mM MES-Tris pH 6.15) for 2 hours at 22 ºC and 100 µE $m^{-2}s^{-1}$ with their abaxial surface facing the buffer solution. Subsequently, either 100 % ethanol, as solvent control, or (+)-ABA dissolved in ethanol was added to a final concentration of 5 µM to

the opening buffer followed by an additional 2 hours incubation. The leaves were then blended with deionized water for approximately 30 seconds using a commercial blender. Epidermal tissues were collected using a 100 μM nylon mesh (Millipore) and rinsed with deionized water. The plant material was dabbed from the mesh onto a microscope slide and covered with a glass coverslip. Images of stomata were acquired using an inverted light microscope (Nikon Eclipse TS100) equipped with a 20x objective (20x/0.17 ∞/0.17 WD 2.1) and connected to the Scion camera and Scion VisiCapture Application Version1.3 (Scion Corporation). For each experiment at least 20 stomata apertures were measured using Fiji. Data represent normalized averages ± s.e.m of three to five experiments.

4.3. Subcellular localization and BiFC analyses

For subcellular localization analyses coding sequences of PP2As without stop codon were inserted into plant binary vectors harboring a pGPTVII.bar backbone (Walter et al., 2004), an expression cassette consisting of the pUBQ10 promoter (AT4G05310; Norris et al., 1993; Krebs et al., 2011) and the HSP18.2 terminator (T) (AT5G59720; Nagaya et al., 2009) and either mTurquoise (Goedhart et al., 2010) located 5' or mVenus (Nagai et al., 2002) located 3' of the multiple cloning site. Constructs for BiFC analyses were generated by ligation of coding sequences into hygII-SPYNE(R) and kanII-SPYCE(MR) plasmids (Waadt et al., 2008). Details of primers and constructs generated are given in Table S1 and Table S2. Plasmids were transformed into *Agrobacterium tumefaciens* GV3101 (pMP90; Koncz and Schell, 1986) and infiltrated together with the

p19 silencing suppressor (Voinnet et al., 2003) into leaves of 5-6 week old *Nicotiana benthamiana* plants as described (Waadt et al., 2013 in press).

Sub-cellular localizations and BiFC analyses were performed by confocal microscopy using a Nikon Eclipse TE2000-U microscope equipped with Nikon Plan 20x/0.40 ∞/0.17 WD 1.3 and Plan Apo 60x/1.20 WI ∞/0.15-0.18 WD 0.22 objectives, a Photometrics CascadeII 512 camera, a MFC2000 z-motor (Applied Scientific Instruments), a QLC-100 spinning disc (VisiTech international), a CL-2000 Diode pumped crystal laser (LaserPhysics Inc.), a LS 300 Kr/Ar laser (Dynamic Laser) and guided by Metamorph software version 7.7.7.0 (Molecular Devices). Images were analyzed and processed in Fiji (Schindelin et al., 2012). Qualitative images are given as maximum projections of 32-plane z-stacks. Images for quantitative BiFC analyses were acquired using the 20x objective as described (Waadt et al., 2013 in press). Data represent average emission values +/- s.e.m. off ten images after subtraction of the p19 background control.

4.4. Co-immunopreciptation analyses

The coding sequence of OST1 was inserted into the pGPTVII.bar plant expression vector harboring a pUBQ10 promoter and NosT expression cassette (see above and Walter et al., 2004) and a 6xHis-3xFLAG (HF)-epitope-tag 3' of the multiple cloning site (kindly providen by Dmitri A. Nusinov (Washington University, St. Louis). The OST1-HF construct was inserted into *A. tumefaciens* and infiltrated together with mTurquoise and mTurquoise-PP2A or mVenus-PP2AC3 and the p19 strain into *N. benthamiana* leaves. Three days after infiltration leaves were harvested and incubated for 1 h in 0.5

MS media. Subsequently, media was exchanged by 0.5 MS + 200 mM sorbitol media and incubated for one additional hour to activate OST1. After treatments, leaf samples were harvested in liquid N_2 and extracted in SII-buffer (100 mM NaPhosphate, pH 8.0, 150 mM NaCl, 5 mM EDTA, 5 mM EGTA, 0.1 % Triton -X-100) supplemented with protease inhibitor (Roche), Phosphatase inhibitors 2 and 3 (Sigma) and 1 mM phenylmethylsulfonyl fluoride (PMSF). After 10 min of rotation at 4 °C samples were sonicated followed by 20 min centrifugation at 16000 *g* and filtration through a 0.45 syringe filter. Protein extracts were mixed with (1/100 v/v) Anti-FLAG M2 magnetic beads equilibrated in SII-buffer and rotated 4 h at 4 °C. Proteins bound to the Anti-FLAG M2 magnetic beads were concentrated using the DynaMag-2 magnetic particle concentrator (Invitrogen) and washed four times in SII-buffer, followed by two washes in FLAG-to-His-buffer (100 mM NaPhosphate, pH 8.0, 150 mM NaCl, 0.05 % Triton-X-100). Proteins were eluted four times in one bead volume of FLAG-to-His-buffer supplemented with 500 µg/mL 3x FLAG peptide (Sigma) and stored at -80 °C. The protein purification protocol was kindly provided by Dmitri A. Nusinov (Washington University, St. Louis). Western-blot and immunodetection was performed after Waadt et al (2013, in press) using a mouse Anti-FLAG M2 antibody (Sigma) or rabbit monoclonal anti-GFP antibody (Invitrogen) followed by a secondary goat anti mouse or anti rabbit IgG (H + L) horseradish peroxidase-conjugate antibody (BioRad).

4.5. Yeast-two-hybrid analyses

Coding sequences were inserted into pGBT9.BS and pGAD.GH vectors (Table S1 and Table S2; Elledge et al., 1991). PJ69-4A yeast strain (James et al., 1996) grown at 28

ºC in YPD media [2% Bactopeptone (BD Biosciences, http://www.bd.com), 1 % yeast extract, 2 % glucose, and 2 % bactoagar] was transformed using the polyethylene glycol/lithium acetate method (Gietz et al., 1992) and plated on CSM agar media (3.35 % YNB=Yeast Nitrogen Base/$(NH_4)_2SO_4$, 0.32 % CSM-Leu-Trp, 2 % glucose, 20 % bactoagar) lacking leucine and tryptophan and incubated for 2-3 days at 28 ºC.

Successfully transformed yeast colonies were re-streaked to new CSM-Leu-Trp plates and incubated over night at 28 ºC. The following day 5 µL of ten-fold dilution series ($OD_{600\ nm}$ of 10^0 - 10^{-4} in 2 % glucose) of transformants were spotted on CSM-Leu-Trp plates as a control and on CSM-Leu-Trp-His plates lacking leucine, tryptophan, and histidine and supplemented with 2.5 mM 3-amino-1,2,4-triazole (3-AT) for selection of positive interaction. Yeast transformants were incubated for 5-7 days at 28 ºC and images were acquired for documentation.

5. REFERENCES

Acharya B, Assmann S. (2009). Hormone interactions in stomatal function. *Plant Molecular Biology* **69**, 451-462.

Abeles F B, Morgan P W, Saltveit M E. (1992). Ethylene in Plant Biology, 2nd edn. New York: Academic Press.

Ahn CS, Han JA, Lee HS, Lee S, Pai HS. (2011). The PP2A regulatory subunit Tap46, a component of the TOR signaling pathway, modulates growth and metabolism in plants. *Plant Cell* **23**, 185-209.

Antolín-Llovera M, Leivar P, Arró M, Ferrer A, Boronat A, Campos N. (2011). Modulation of plant HMG-CoA reductase by protein phosphatase 2A: positive and negative control at a key node of metabolism. *Plant Signal Behav* **6**, 1127-31.

Ariño J, Pérez-Callejón E, Cunillera N, Camps M, Posas F, Ferrer A. (1993). Protein phosphatases in higher plants: multipli-city of type 2A phosphatases in *Arabidopsis thaliana*. *Plant Mol. Biol* **21,** 475-485.

Ballesteros I, Domínguez T, Sauer M, Paredes P, Duprat A, Rojo E, Sanmartín M, Sánchez-Serrano JJ. (2012). Specialised functions of the PP2A subfamily II catalytic subunits PP2A-C3 and PP2A-C4 in the distribution of auxin fluxes and development in Arabidopsis. *Plant J*.

Blakeslee JJ, Zhou HW, Heath JT, Skottke KR, Barrios JA, Liu SY, Delong A. (2008). Specificity of RCN1-mediated protein phosphatase 2A regulation in meristem organization and stress response in roots. *Plant Physiol* **146**, 539-53.

Boudsocq M, Barbier-Brygoo H, Laurière C. (2004). Identification of nine sucrose nonfermenting 1-related protein kinases 2 activated by hyperosmotic and saline stresses in Arabidopsis thaliana. *J Biol Chem* **279**, 41758-66.

Brandt B, Brodsky DE, Xue S, Negi J, Iba K, Kangasjärvi J, Ghassemian M, Stephan AB, Hu H, Schroeder JI. (2012). Reconstitution of abscisic acid activation of SLAC1 anion channel by CPK6 and OST1 kinases and branched ABI1 PP2C phosphatase action. *Proc Natl Acad Sci U S A* **109**, 10593-8.

Camilleri C, Azimzadeh J, Pastuglia M, Bellini C, Grandjean O, Bouchez D. (2002). The Arabidopsis TONNEAU2 gene encodes a putative novel protein phosphatase 2A regulatory subunit essential for the control of the cortical cytoskeleton. *Plant Cell* **14**, 833-45.

Casamayor A, Perez-Callejon E, Pujol G, Arino J, Ferrer A. (1994). Molecular characterization of a fourth isoform of the catalytic subunit of protein phosphatase 2A from *Arabidopsis thaliana*. *Plant Mol. Biol* **26**, 523-528.

Corum JW, Hartung AJ, Stamey RT, Rundle SJ. (1996). Characterization of DNA sequences encoding a novel isoform of the 55 kDa B regulatory subunit of the type 2A protein serine/threonine phosphatase of Arabidopsis thaliana. *Plant Mol Biol* **31**, 419-27.

Dai M, Terzaghi W, Wang H. (2012). Multifaceted roles of Arabidopsis PP6 phosphatase in regulating cellular signaling and plant development. *Plant Signal Behav* **8**.

Deak KI, Malamy J. (2005). Osmotic regulation of root system architecture. *Plant J* **43**, 17-28.

Delong A. (2006). Switching the flip: protein phosphatase roles in signaling pathways. *Curr Opin Plant Biol* **9**, 470-7.

Depaoli-Roach AA, Park IK, Cerovsky V, Csortos C, Durbin SD, Kuntz MJ, Sitikov A, Tang PM, Verin A, Zolnierowicz S. (1994). Serine/threonine protein phosphatases in the control of cell function. *Adv Enzyme Regul* **34**, 199-224.

Deruère J, Jackson K, Garbers C, Söll D, Delong A. (1999). The RCN1-encoded A subunit of protein phosphatase 2A increases phosphatase activity in vivo. *Plant J* **20**, 389-99.

De Smet I, Vanneste S, Inzé D, Beeckman T. (2006). Lateral root initiation or the birth of a new meristem. *Plant Mol Biol* **60**, 871-87.

Di Rubbo S, Irani NG, Russinova E. (2011). PP2A phosphatases: the "on-off" regulatory switches of brassinosteroid signaling. *Sci Signal* **4**, pe25.

Duan CG, Fang YY, Zhou BJ, Zhao JH, Hou WN, Zhu H, Ding SW, Guo HS. (2012). Suppression of Arabidopsis ARGONAUTE1-mediated slicing, transgene-induced RNA silencing, and DNA methylation by distinct domains of the Cucumber mosaic virus 2b protein. *Plant Cell* **24**, 259-74.

Elledge SJ, Mulligan JT, Ramer SW, Spottswood M, Davis RW. (1991). Lambda YES: a multifunctional cDNA expression vector for the isolation of genes by complementation of yeast and Escherichia coli mutations. *Proc Natl Acad Sci U S A* **88**, 1731-5.

Farkas I, Dombrádi V, Miskei M, Szabados L, Koncz C. (2007). Arabidopsis PPP family of serine/threonine phosphatases. *Trends Plant Sci* **12**, 169-76.

Fields S, Sternglanz R. (1994). The two-hybrid system: an assay for protein-protein interactions. *Trends Genet* **10**, 286-92.

Finkelstein R, Reeves W, Ariizumi T, Steber C. (2008). Molecular aspects of seed dormancy. *Annu Rev Plant Biol* **59**, 387-415.

Fisher RH, Barton MK, Cohen JD, Cooke TJ. (1996). Hormonal Studies of fass, an Arabidopsis Mutant That Is Altered in Organ Elongation. *Plant Physiol* **110**, 1109-21.

Fujii H, Chinnusamy V, Rodrigues A, Rubio S, Antoni R, Park SY, Cutler SR, Sheen J, Rodriguez PL, Zhu JK. (2009). In vitro reconstitution of an abscisic acid signalling pathway. *Nature* **462**, 660-4.

Fuji K, Shimada T, Takahashi H, Tamura K, Koumoto Y, Utsumi S, Nishizawa K, Maruyama N, Hara-Nishimura I. (2007). Arabidopsis vacuolar sorting mutants (green fluorescent seed) can be identified efficiently by secretion of vacuole-targeted green fluorescent protein in their seeds. *Plant Cell* **19**, 597-609.

Fujii H, Zhu JK. (2009). Arabidopsis mutant deficient in 3 abscisic acid-activated protein kinases reveals critical roles in growth, reproduction, and stress. *Proc Natl Acad Sci U S A* **106**, 8380-5.

Gao X, Nagawa S, Wang G, Yang Z. (2008). Cell polarity signaling: focus on polar auxin transport. *Mol Plant* **1**, 899-909.

Garbers C, Delong A, Deruére J, Bernasconi P, Söll D. (1996). A mutation in protein phosphatase 2A regulatory subunit A affects auxin transport in Arabidopsis. *EMBO J* **15**, 2115-24.

Geiger D, Scherzer S, Mumm P, Stange A, Marten I, Bauer H, Ache P, Matschi S, Liese A, Al-Rasheid KA, Romeis T, Hedrich R. (2009). Activity of guard cell anion channel SLAC1 is controlled by drought-stress signaling kinase-phosphatase pair. *Proc Natl Acad Sci U S A* **106**, 21425-30.

Gietz D, St Jean A, Woods RA, Schiestl RH. (1992). Improved method for high efficiency transformation of intact yeast cells. *Nucleic Acids Res* **20**, 1425.

Goedhart J, Van Weeren L, Hink MA, Vischer NO, Jalink K, Gadella TW, Jr. (2010). Bright cyan fluorescent protein variants identified by fluorescence lifetime screening. *Nat Methods* **7**, 137-9.

Hayashi Y, Nakamura S, Takemiya A, Takahashi Y, Shimazaki K, Kinoshita T. (2010). Biochemical characterization of in vitro phosphorylation and dephosphorylation of the plasma membrane H+-ATPase. *Plant Cell Physiol* **51**, 1186-96.

Haynes JG, Hartung AJ, Hendershot JD, Passingham RS, Rundle SJ. (1999).

Molecular characterization of the B' regulatory subunit gene family of Arabidopsis protein phosphatase 2A. *Eur J Biochem* **260**, 127-36.

Heidari B, Matre P, Nemie-Feyissa D, Meyer C, Rognli OA, Møller SG, Lillo C. (2011). Protein phosphatase 2A B55 and A regulatory subunits interact with nitrate reductase and are essential for nitrate reductase activation. *Plant Physiol* **156**, 165-72.

Himmelbach A, Iten M, Grill E. (1998). Signalling of abscisic acid to regulate plant growth. *Philos Trans R Soc Lond B Biol Sci* **353**, 1439-44.

Hubbard KE, Nishimura N, Hitomi K, Getzoff ED, Schroeder JI. (2010). Early abscisic acid signal transduction mechanisms: newly discovered components and newly emerging questions. *Genes Dev* **24**, 1695-708.

James P, Halladay J, Craig EA. (1996). Genomic libraries and a host strain designed for highly efficient two-hybrid selection in yeast. *Genetics* **144**, 1425-36.

Janssens V, Goris J. (2001). Protein phosphatase 2A: a highly regulated family of serine/threonine phosphatases implicated in cell growth and signalling. *Biochem J* **353**, 417-39.

Kerppola TK. (2006). Design and implementation of bimolecular fluorescence complementation (BiFC) assays for the visualization of protein interactions in living cells. *Nat Protoc* **1**, 1278-86.

Kim TH, Böhmer M, Hu H, Nishimura N, Schroeder JI. (2010). Guard cell signal transduction network: advances in understanding abscisic acid, CO_2, and Ca^{2+} signaling. *Annu Rev Plant Biol* **61**, 561-91.

Kirik A, Ehrhardt DW, Kirik V. (2012). TONNEAU2/FASS regulates the geometry of microtubule nucleation and cortical array organization in interphase Arabidopsis cells. *Plant Cell* **24**, 1158-70.

Kobayashi Y, Murata M, Minami H, Yamamoto S, Kagaya Y, Hobo T, Yamamoto A, Hattori T. (2005). Abscisic acid-activated SNRK2 protein kinases function in the gene-regulation pathway of ABA signal transduction by phosphorylating ABA response element-binding factors. *Plant J* **44**, 939-949.

Krebs M, Held K, Binder A, Hashimoto K, Den Herder G, Parniske M, Kudla J, Schumacher K. (2012). FRET-based genetically encoded sensors allow high-resolution live cell imaging of Ca(2)(+) dynamics. *Plant J* **69**, 181-92.

Kremmer E, Ohst K, Kiefer J, Brewis N, Walter G. (1997). Separation of PP2A core enzyme and holoenzyme with monoclonal antibodies against the regulatory A

subunit: abundant expression of both forms in cells. *Mol Cell Biol* **17**, 1692-701.

Kwak JM, Moon JH, Murata Y, Kuchitsu K, Leonhardt N, Delong A, Schroeder JI. (2002). Disruption of a guard cell-expressed protein phosphatase 2A regulatory subunit, RCN1, confers abscisic acid insensitivity in Arabidopsis. *Plant Cell* **14**, 2849-61.

Larsen PB, Cancel JD. (2003). Enhanced ethylene responsiveness in the Arabidopsis eer1 mutant results from a loss-of-function mutation in the protein phosphatase 2A A regulatory subunit, RCN1. *Plant J* **34**, 709-18.

Latorre KA, Harris DM, Rundle SJ. (1997). Differential expression of three Arabidopsis genes encoding the B' regulatory subunit of protein phosphatase 2A. *Eur J Biochem* **245**, 156-63.

Leivar P, Antolín-Llovera M, Ferrero S, Closa M, Arró M, Ferrer A, Boronat A, Campos N. (2011). Multilevel control of Arabidopsis 3-hydroxy-3-methylglutaryl coenzyme A reductase by protein phosphatase 2A. *Plant Cell* **23**, 1494-511.

Li J, Chory J. (1997). A putative leucine-rich repeat receptor kinase involved in brassinosteroid signal transduction. *Cell* **90**, 929-38.

Lizotte DL, Blakeslee JJ, Siryaporn A, Heath JT, Delong A. (2008). A PP2A active site mutant impedes growth and causes misregulation of native catalytic subunit expression. *J Cell Biochem* **103**, 1309-25.

Luo J, Shen G, Yan J, He C, Zhang H. (2006). AtCHIP functions as an E3 ubiquitin ligase of protein phosphatase 2A subunits and alters plant response to abscisic acid treatment. *Plant J* **46**, 649-57.

Ma Y, Szostkiewicz I, Korte A, Moes D, Yang Y, Christmann A, Grill E. (2009). Regulators of PP2C phosphatase activity function as abscisic acid sensors. *Science* **324**, 1064-8.

Matre P, Meyer C, Lillo C. (2009). Diversity in subcellular targeting of the PP2A B'eta subfamily members. *Planta* **230**, 935-45.

McClinton RS, Sung ZR. (1997). Organization of cortical microtubules at the plasma membrane in Arabidopsis. *Planta* **201**, 252-60.

Merlot S, Mustilli AC, Genty B, North H, Lefebvre V, Sotta B, Vavasseur A, Giraudat J. (2002). Use of infrared thermal imaging to isolate Arabidopsis mutants defective in stomatal regulation. *Plant J* **30**, 601-9.

Michniewicz M, Zago MK, Abas L, Weijers D, Schweighofer A, Meskiene I, Heisler MG, Ohno C, Zhang J, Huang F, Schwab R, Weigel D, Meyerowitz EM, Luschnig C, Offringa R, Friml J. (2007). Antagonistic regulation of PIN phosphorylation by PP2A and PINOID directs auxin flux. *Cell* **130**, 1044-56.

Moorhead GB, De Wever V, Templeton G, Kerk D. (2009). Evolution of protein phosphatases in plants and animals. *Biochem J* **417**, 401-9.

Muday GK, Brady SR, Argueso C, Deruère J, Kieber JJ, Delong A. (2006). RCN1-regulated phosphatase activity and EIN2 modulate hypocotyl gravitropism by a mechanism that does not require ethylene signaling. *Plant Physiol* **141**, 1617-29.

Mustilli AC, Merlot S, Vavasseur A, Fenzi F, Giraudat J. (2002). Arabidopsis OST1 protein kinase mediates the regulation of stomatal aperture by abscisic acid and acts upstream of reactive oxygen species production. *Plant Cell* **14**, 3089-99.

Nagai T, Ibata K, Park ES, Kubota M, Mikoshiba K, Miyawaki A. (2002). A variant of yellow fluorescent protein with fast and efficient maturation for cell-biological applications. *Nat Biotechnol* **20**, 87-90.

Nagaya S, Kawamura K, Shinmyo A, Kato K. (2010). The HSP terminator of Arabidopsis thaliana increases gene expression in plant cells. *Plant Cell Physiol* **51**, 328-32.

Nakagawa M, Shimamoto K, Kyozuka J. (2002). Overexpression of RCN1 and RCN2, rice TERMINAL FLOWER 1/CENTRORADIALIS homologs, confers delay of phase transition and altered panicle morphology in rice. *Plant J* **29**, 743-50.

Nishimura N, Hitomi K, Arvai AS, Rambo RP, Hitomi C, Cutler SR, Schroeder JI, Getzoff ED. (2009). Structural mechanism of abscisic acid binding and signaling by dimeric PYR1. *Science* **326**, 1373-9.

Nishimura N, Sarkeshik A, Nito K, Park SY, Wang A, Carvalho PC, Lee S, Caddell DF, Cutler SR, Chory J, Yates JR, Schroeder JI. (2010). PYR/PYL/RCAR family members are major in-vivo ABI1 protein phosphatase 2C-interacting proteins in Arabidopsis. *Plant J* **61**, 290-9.

Norris SR, Meyer SE, Callis J. (1993). The intron of Arabidopsis thaliana polyubiquitin genes is conserved in location and is a quantitative determinant of chimeric gene expression. *Plant Mol Biol* **21**, 895-906.

País SM, García MN, Téllez-Iñón MT, Capiati DA. (2010). Protein phosphatases type 2A mediate tuberization signaling in Solanum tuberosum L. leaves. *Planta* **232**, 37-49.

Park SY, Fung P, Nishimura N, Jensen DR, Fujii H, Zhao Y, Lumba S, Santiago J, Rodrigues A, Chow TF, Alfred SE, Bonetta D, Finkelstein R, Provart NJ, Desveaux D, Rodriguez PL, Mccourt P, Zhu JK, Schroeder JI, Volkman BF, Cutler SR. (2009). Abscisic acid inhibits type 2C protein phosphatases via the PYR/PYL family of START proteins. *Science* **324**, 1068-71.

Pernas M, García-Casado G, Rojo E, Solano R, Sánchez-Serrano JJ. (2007). A protein phosphatase 2A catalytic subunit is a negative regulator of abscisic acid signalling. *Plant J* **51**, 763-78.

Price NE, Mumby MC. (2000). Effects of Regulatory Subunits on the Kinetics of Protein Phosphatase 2A. *Biochemistry* **37**, 11312-11318.

Rashotte AM, Delong A, Muday GK. (2001). Genetic and chemical reductions in protein phosphatase activity alter auxin transport, gravity response, and lateral root growth. *Plant Cell* **13**, 1683-97.

Rodriguez-Gacio C, Matilla-Vasquez MA, Matilla AJ. (2009). Seed dormancy and ABA signaling: the breakthrough goes on. *Plant Signaling Behav* **11**, 1035-49.

Ruediger R, Hentz M, Fait J, Mumby M, Walter G. (1994). Molecular model of the A subunit of protein phosphatase 2A: interaction with other subunits and tumor antigens. *J Virol* **68**, 123-9.

Saito N, Munemasa S, Nakamura Y, Shimoishi Y, Mori IC, Murata Y. (2008). Roles of RCN1, regulatory A subunit of protein phosphatase 2A, in methyl jasmonate signaling and signal crosstalk between methyl jasmonate and abscisic acid. *Plant Cell Physiol* **49**, 1396-401.

Santiago J, Rodrigues A, Saez A, Rubio S, Antoni R, Dupeux F, Park SY, Marquez JA, Cutler SR, Rodriguez PL. (2009). Modulation of drought resistance by the abscisic acid receptor PYL5 through inhibition of clade A PP2Cs. *Plant J* **60**, 575-88.

Santner A, Calderon-Villalobos LI, Estelle M. (2009). Plant hormones are versatile chemical regulators of plant growth. *Nat Chem Biol* **5**, 301-7.

Sato A, Sato Y, Fukao Y, Fujiwara M, Umezawa T, Shinozaki K, Hibi T, Taniguchi M, Miyake H, Goto DB, Uozumi N. (2009). Threonine at position 306 of the KAT1 potassium channel is essential for channel activity and is a target site for ABA-activated SnRK2/OST1/SnRK2.6 protein kinase. *Biochem J* **424**, 439-48.

Schindelin J, Arganda-Carreras I, Frise E, Kaynig V, Longair M, Pietzsch T, Preibisch S, Rueden C, Saalfeld S, Schmid B, Tinevez JY, White DJ, Hartenstein V, Eliceiri K, Tomancak P, Cardona A. (2012). Fiji: an open-

source platform for biological-image analysis. *Nat Methods* **9**, 676-82.

Schlücking K, Edel KH, Köster P, Drerup MM, Eckert C, Steinhorst L, Waadt R, Batistic O, Kudla J. (2013). A New β-Estradiol-Inducible Vector Set that Facilitates Easy Construction and Efficient Expression of Transgenes Reveals CBL3-Dependent Cytoplasm to Tonoplast Translocation of CIPK5. *Mol Plant*.

Schroeder JI, Allen GJ, Hugouvieux V, Kwak JM, Waner D. (2001). Guard Cell Signal Transduction. *Annu Rev Plant Physiol Plant Mol Biol* **52**, 627-58.

Sents W, Ivanova E, Lambrecht C, Haesen D, Janssens V. (2012). The biogenesis of active protein phosphatase 2A holoenzymes: a tightly regulated process creating phosphatase specificity. *FEBS J*.

Shi Y. (2009). Assembly and structure of protein phosphatase 2A. *Sci China C Life Sci* **52**, 135-46.

Sirichandra C, Davanture M, Turk BE, Zivy M, Valot B, Leung J, Merlot S. (2010). The Arabidopsis ABA-activated kinase OST1 phosphorylates the bZIP transcription factor ABF3 and creates a 14-3-3 binding site involved in its turnover. *PLoS One* **5**, e13935.

Sirichandra C, Gu D, Hu HC, Davanture M, Lee S, Djaoui M, Valot B, Zivy M, Leung J, Merlot S, Kwak JM. (2009). Phosphorylation of the Arabidopsis AtrbohF NADPH oxidase by OST1 protein kinase. *FEBS Lett* **583**, 2982-6.

Sirichandra C, Wasilewska A, Vlad F, Valon C, Leung J. (2009). The guard cell as a single-cell model towards understanding drought tolerance and abscisic acid action. *J Exp Bot* **60**, 1439-63.

Skottke KR, Yoon GM, Kieber JJ, Delong A. (2011). Protein phosphatase 2A controls ethylene biosynthesis by differentially regulating the turnover of ACC synthase isoforms. *PLoS Genet* **7**, e1001370.

Sukumar P, Edwards KS, Rahman A, Delong A, Muday GK. (2009). PINOID kinase regulates root gravitropism through modulation of PIN2-dependent basipetal auxin transport in Arabidopsis. *Plant Physiol* **150**, 722-35.

Tang W, Yuan M, Wang R, Yang Y, Wang C, Oses-Prieto JA, Kim TW, Zhou HW, Deng Z, Gampala SS, Gendron JM, Jonassen EM, Lillo C, Delong A, Burlingame AL, Sun Y, Wang ZY. (2011). PP2A activates brassinosteroid-responsive gene expression and plant growth by dephosphorylating BZR1. *Nat Cell Biol* **13**, 124-31.

Terol J, Bargues M, Carrasco P, Pérez-Alonso M, Paricio N. (2002). Molecular characterization and evolution of the protein phosphatase 2A B' regulatory

subunit family in plants. *Plant Physiol* **129**, 808-22.

Testerink C, Dekker HL, Lim ZY, Johns MK, Holmes AB, Koster CG, Ktistakis NT, Munnik T. (2004). Isolation and identification of phosphatidic acid targets from plants. *Plant J* **39**, 527-36.

Torres-Ruiz RA, Jürgens G. (1994). Mutations in the FASS gene uncouple pattern formation and morphogenesis in Arabidopsis development. *Development* **120**, 2967-78.

Tran HT, Nimick M, Uhrig RG, Templeton G, Morrice N, Gourlay R, Delong A, Moorhead GB. (2012). Arabidopsis thaliana histone deacetylase 14 (HDA14) is an α-tubulin deacetylase that associates with PP2A and enriches in the microtubule fraction with the putative histone acetyltransferase ELP3. *Plant J* **71**, 263-72.

Trotta A, Wrzaczek M, Scharte J, Tikkanen M, Konert G, Rahikainen M, Holmström M, Hiltunen HM, Rips S, Sipari N, Mulo P, Weis E, Von Schaewen A, Aro EM, Kangasjärvi S. (2011). Regulatory subunit B'gamma of protein phosphatase 2A prevents unnecessary defense reactions under low light in Arabidopsis. *Plant Physiol* **156**, 1464-80.

Tseng TS, Briggs WR. (2010). The Arabidopsis *rcn1* mutation impairs dephosphorylation of Phot2, resulting in enhanced blue light responses. *Plant Cell* **22**, 392-402.

Umezawa T, Sugiyama N, Mizoguchi M, Hayashi S, Myouga F, Yamaguchi-Shinozaki K, Ishihama Y, Hirayama T, Shinozaki K. (2009). Type 2C protein phosphatases directly regulate abscisic acid-activated protein kinases in Arabidopsis. *Proc Natl Acad Sci U S A* **106**, 17588-93.

Vlad F, Rubio S, Rodrigues A, Sirichandra C, Belin C, Robert N, Leung J, Rodriguez PL, Laurière C, Merlot S. (2009). Protein phosphatases 2C regulate the activation of the Snf1-related kinase OST1 by abscisic acid in Arabidopsis. *Plant Cell* **21**, 3170-84.

Voinnet O, Rivas S, Mestre P, Baulcombe D. (2003). An enhanced transient expression system in plants based on suppression of gene silencing by the p19 protein of tomato bushy stunt virus. *Plant J* **33**, 949-56.

Waadt R, Schmidt LK, Lohse M, Hashimoto K, Bock R, Kudla J. (2008). Multicolor bimolecular fluorescence complementation reveals simultaneous formation of alternative CBL/CIPK complexes in planta. *Plant J* **56**, 505-16.

Walter M, Chaban C, Schutze K, Batistic O, Weckermann K, Nake C, Blazevic D,

Grefen C, Schumacher K, Oecking C, Harter K, Kudla J. (2004). Visualization of protein interactions in living plant cells using bimolecular fluorescence complementation. *Plant J* **40**, 428-38.

Weiner H, Stitt M. (1993). Sucrose-phosphate synthase phosphatase, a type 2A protein phosphatase, changes its sensitivity towards inhibition by inorganic phosphate in spinach leaves. *FEBS Lett* **333**, 159-64.

Wen F, Wang J, Xing D. (2012). A protein phosphatase 2A catalytic subunit modulates blue light-induced chloroplast avoidance movements through regulating actin cytoskeleton in Arabidopsis. *Plant Cell Physiol* **53**, 1366-79.

Wilkinson S, Davies W J. (2002). ABA-based chemical signaling: the coordination of responses to stress in plants. *Plant Cell Environ* **25**, 195-210.

Winter D, Vinegar B, Nahal H, Ammar R, Wilson GV, Provart NJ. (2007). An "Electronic Fluorescent Pictograph" browser for exploring and analyzing large-scale biological data sets. *PLoS One* **2**, e718.

Wu G, Wang X, Li X, Kamiya Y, Otegui MS, Chory J. (2011). Methylation of a phosphatase specifies dephosphorylation and degradation of activated brassinosteroid receptors. *Sci Signal* **4**, ra29.

Wuriyanghan H, Zhang B, Cao WH, Ma B, Lei G, Liu YF, Wei W, Wu HJ, Chen LJ, Chen HW, Cao YR, He SJ, Zhang WK, Wang XJ, Chen SY, Zhang JS. (2009). The ethylene receptor ETR2 delays floral transition and affects starch accumulation in rice. *Plant Cell* **21**, 1473-94.

Xu C, Jing R, Mao X, Jia X, Chang X. (2007). A wheat (Triticum aestivum) protein phosphatase 2A catalytic subunit gene provides enhanced drought tolerance in tobacco. *Ann Bot* **99**, 439-50.

Xu J, Li HD, Chen LQ, Wang Y, Liu LL, He L, Wu WH. (2006). A protein kinase, interacting with two calcineurin B-like proteins, regulates K+ transporter AKT1 in Arabidopsis. *Cell* **125**, 1347-60.

Xu Y, Xing Y, Chen Y, Chao Y, Lin Z, Fan E, Yu JW, Strack S, Jeffrey PD, Shi Y. (2006). Structure of the protein phosphatase 2A holoenzyme. *Cell* **127**, 1239-51.

Yoshida T, Fujita Y, Sayama H, Kidokoro S, Maruyama K, Mizoi J, Shinozaki K, Yamaguchi-Shinozaki K. (2010). AREB1, AREB2, and ABF3 are master transcription factors that cooperatively regulate ABRE-dependent ABA signaling involved in drought stress tolerance and require ABA for full activation. *Plant J* **61**, 672-85.

Yoshida R, Hobo T, Ichimura K, Mizoguchi T, Takahashi F, Aronso J, Ecker JR, Shinozaki K. (2002). ABA-activated SnRK2 protein kinase is required for dehydration stress signaling in Arabidopsis. *Plant Cell Physiol* **43**, 1473-83.

Yoshida T, Nishimura N, Kitahata N, Kuromori T, Ito T, Asami T, Shinozaki K, Hirayama T. (2006). ABA-hypersensitive germination3 encodes a protein phosphatase 2C (AtPP2CA) that strongly regulates abscisic acid signaling during germination among Arabidopsis protein phosphatase 2Cs. *Plant Physiol* **140**, 115-26.

Zhang J, Nodzynski T, Pencík A, Rolcík J, Friml J. (2010). PIN phosphorylation is sufficient to mediate PIN polarity and direct auxin transport. *Proc Natl Acad Sci U S A* **107**, 918-22.

Zhou HW, Nussbaumer C, Chao Y, Delong A. (2004). Disparate roles for the regulatory A subunit isoforms in Arabidopsis protein phosphatase 2A. *Plant Cell* **16**, 709-22.

6. SUPPLEMENTAL INFORMATION

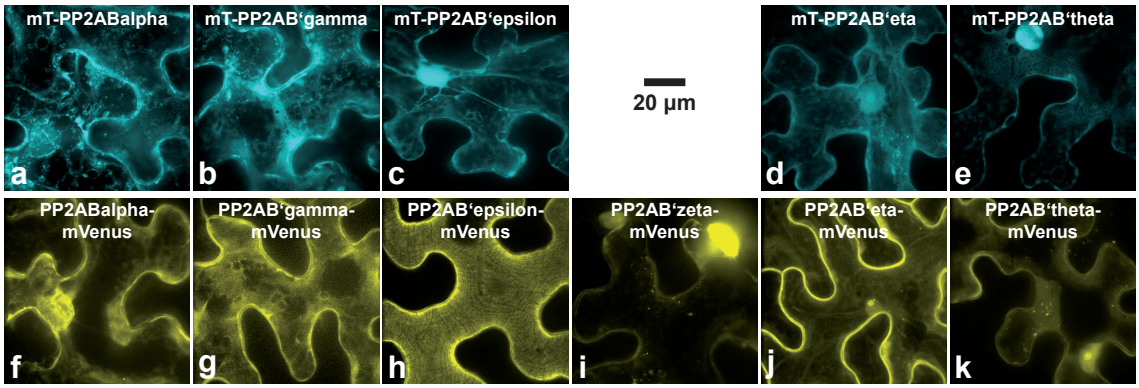

Figure S1. Subcellular localization of PP2AB-subunits. PP2AB constructs were infiltrated into *N. benthamiana* leaves and expressed as an mTurquoise-(mT)-PP2AB (cyan) or a PP2AB-mVenus fusion (yellow). Three days after infiltration 32-z-stack-images were recorded displayed as a maximum projection. The fusion proteins analyzed in images **a-k** and the scale bar are indicated.

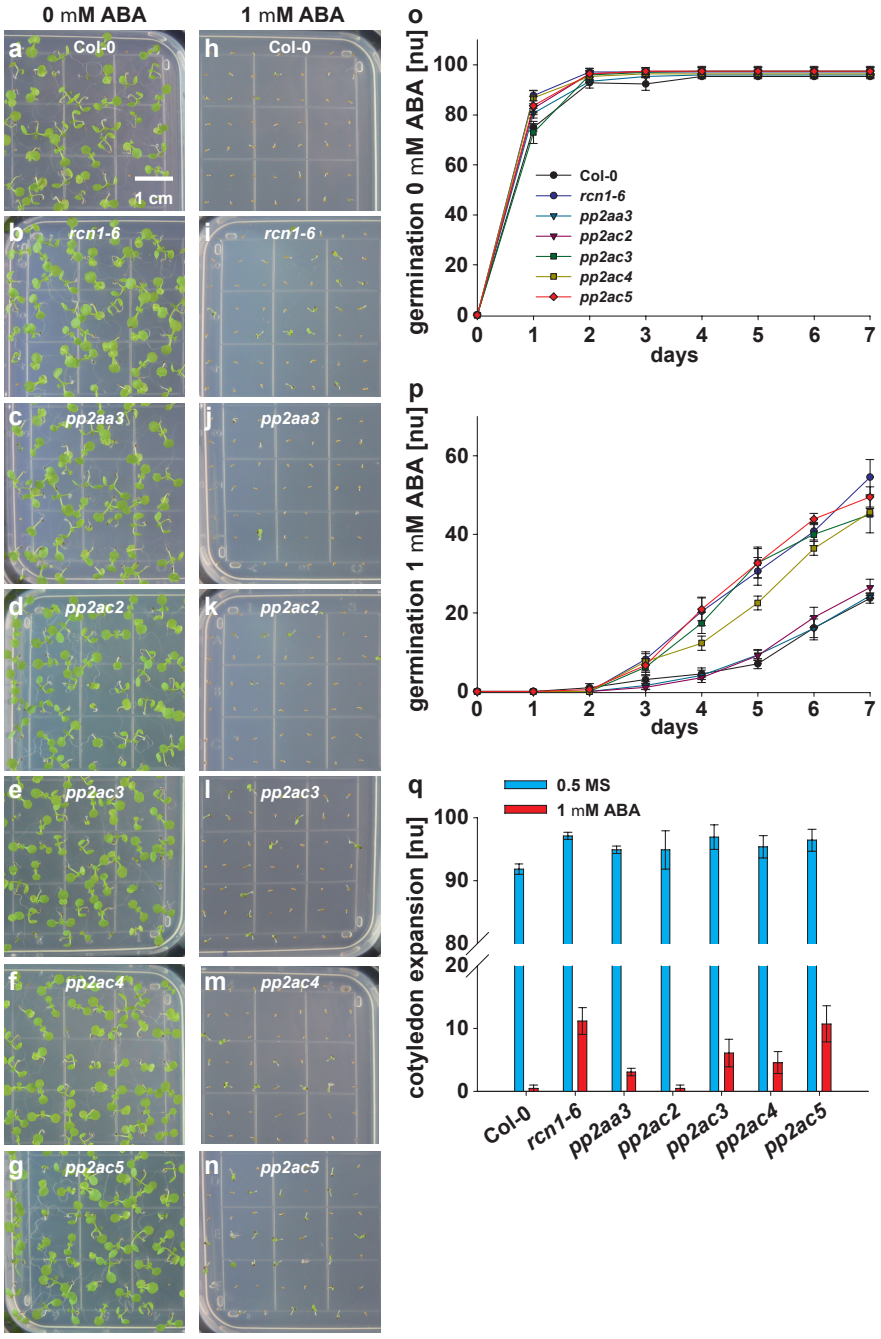

Figure S2. *pp2a* single mutants are slightly ABA hyposensitive in seed germination. Indicated genotypes were grown for seven days in 0.5 MS media (**a-g**) or in 0.5 MS media supplemented with 1 mM ABA (**h-n**). Seed germination on media without ABA (**o**) and media supplemented with 0.5 μM ABA (**p**) was recorded for seven days and cotyledon expansion was recorded on the seventh day (**q**). **o-q**, Normalized averages ± s.e.m of four experiments. Compared to Col-0, *rcn1-6*, *pp2ac3*, *pp2ac4* and *pp2ac5* mutants display slight ABA hyposensitivity in ABA inhibition of seed germination and cotyledon greening/expansion.

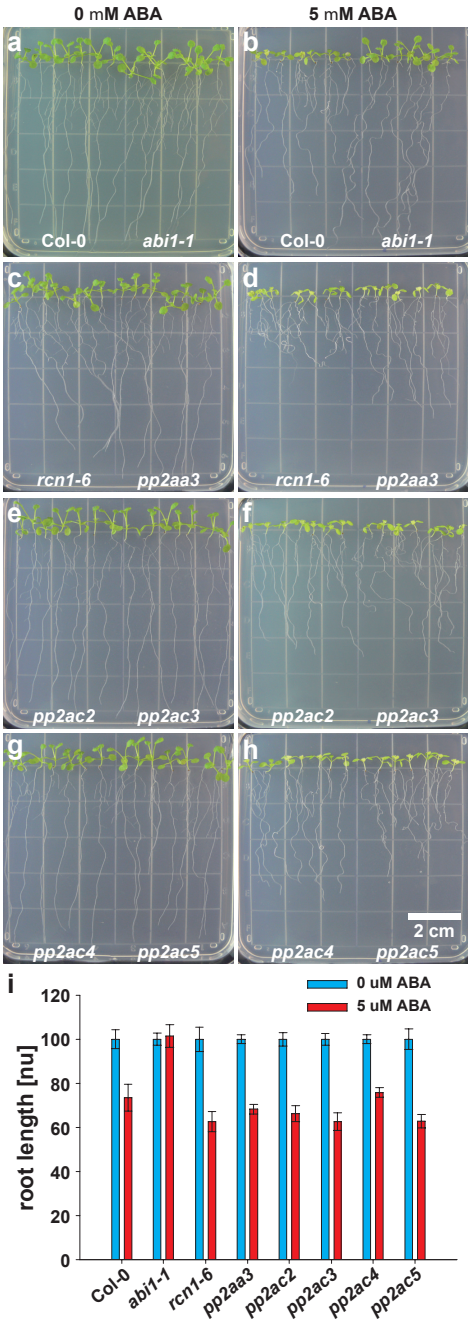

Figure S3. Roots of *rcn1-6* and *pp2ac5* are hypersensitive to ABA. a-h, Four-day-old seedlings of indicated genotypes were transferred to 0.5 MS media without (**a**, **c**, **e, g**) or supplemented with 5 μM ABA (**b**, **d**, **f, h**) and grown for additional five days before images were acquired. **i**, Root length of indicated genotypes five days after transfer to 0.5 MS media ± 5 μM ABA was normalized to the root length in control conditions (0.5 MS). Data represent averages ± s.e.m. of four experiments. Compared to Col-0, *rcn1-6* and *pp2ac5* exhibit an enhanced root curling but no difference in root length in the presence of 5 μM ABA. The ABA insensitive *abi1-1* mutant was used as a control.

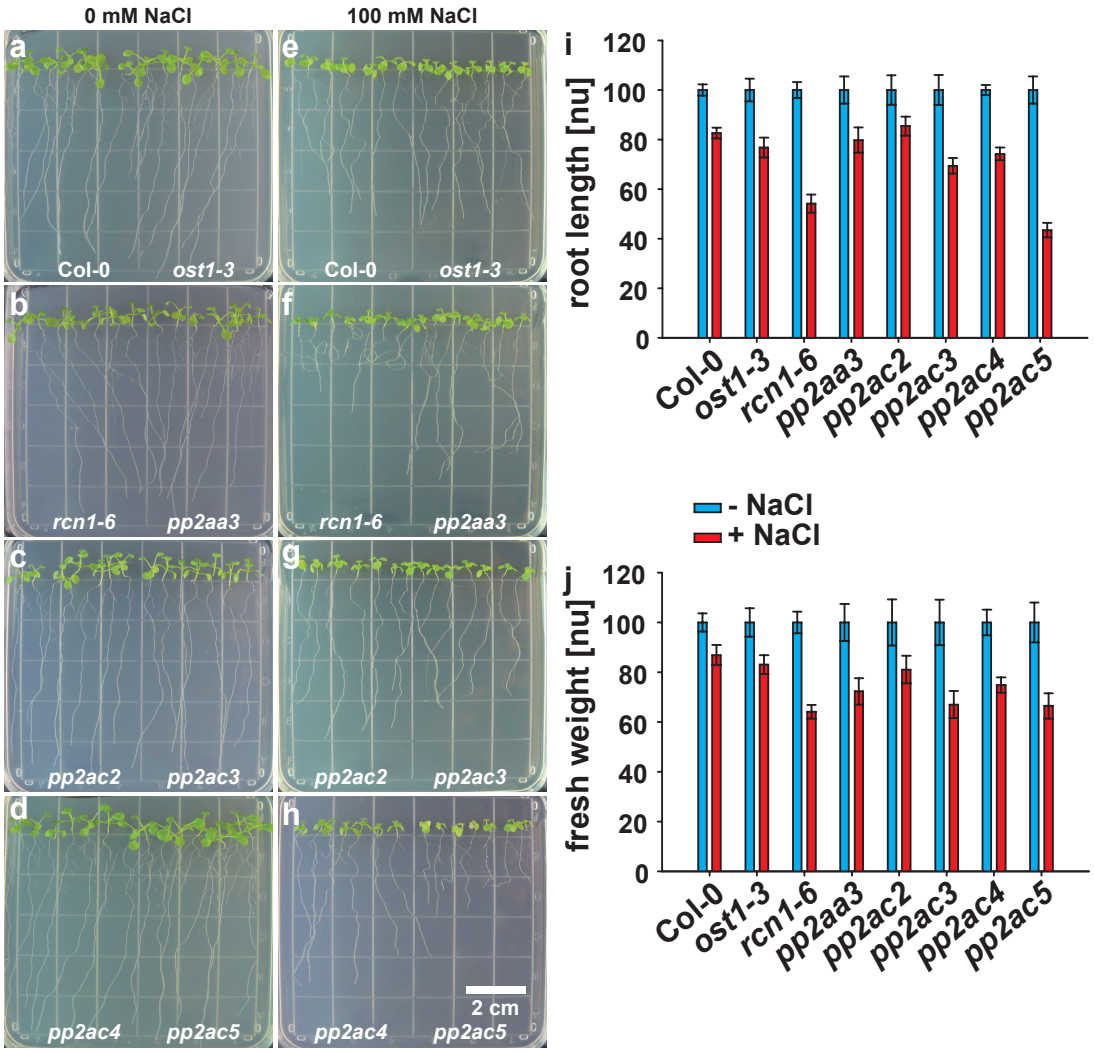

Figure S4. *rcn1-6* and *pp2ac5* are hypersensitive to 100 mM NaCl. Four-day-old seedlings of indicated genotypes were transferred to 0.5 MS media without (**a-d**) or supplemented with 100 mM NaCl (**e-h**) and grown for additional six days before images were acquired. Root length (**i**) and fresh weight (**j**) of indicated genotypes six days after transfer to 0.5 MS media ± 100 mM NaCl were normalized to control conditions (0.5 MS). Data represent averages ± s.e.m. of six experiments.

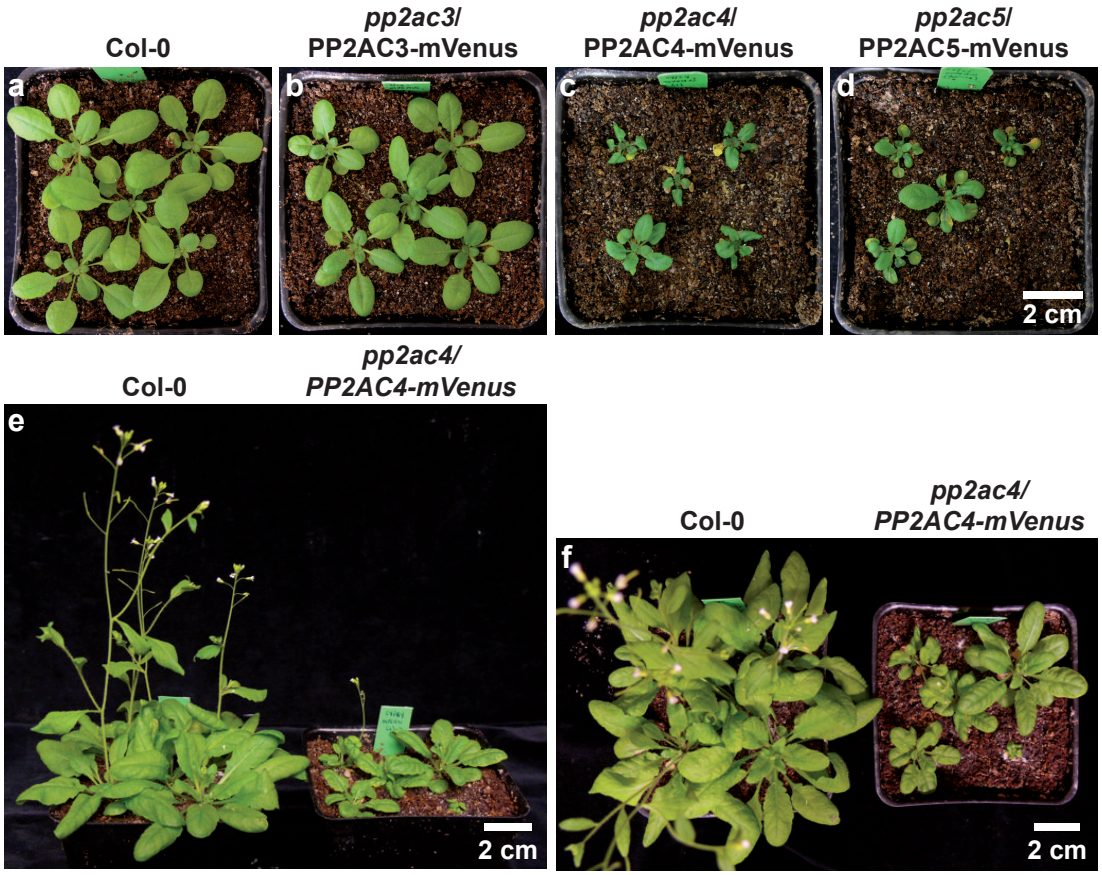

Figure S5. pUBQ10-PP2AC overexpression lines. *PP2AC3* (**b**), *-C4* (**c,e,f**), *-C5* (**d**) were fused to C-terminal mVenus tags and transformed into corresponding mutant background. Overexpression of PP2AC-mVenus constructs affects plant growth and development. Indicated *pp2ac*/PP2AC-mVenus lines compared to wild type Col-0. **a-d**, 29 day-old plants. **e-f**, 42 day-old plants. Note the reduced growth of *pp2ac*/PP2AC-mVenus lines compared to Col-0.

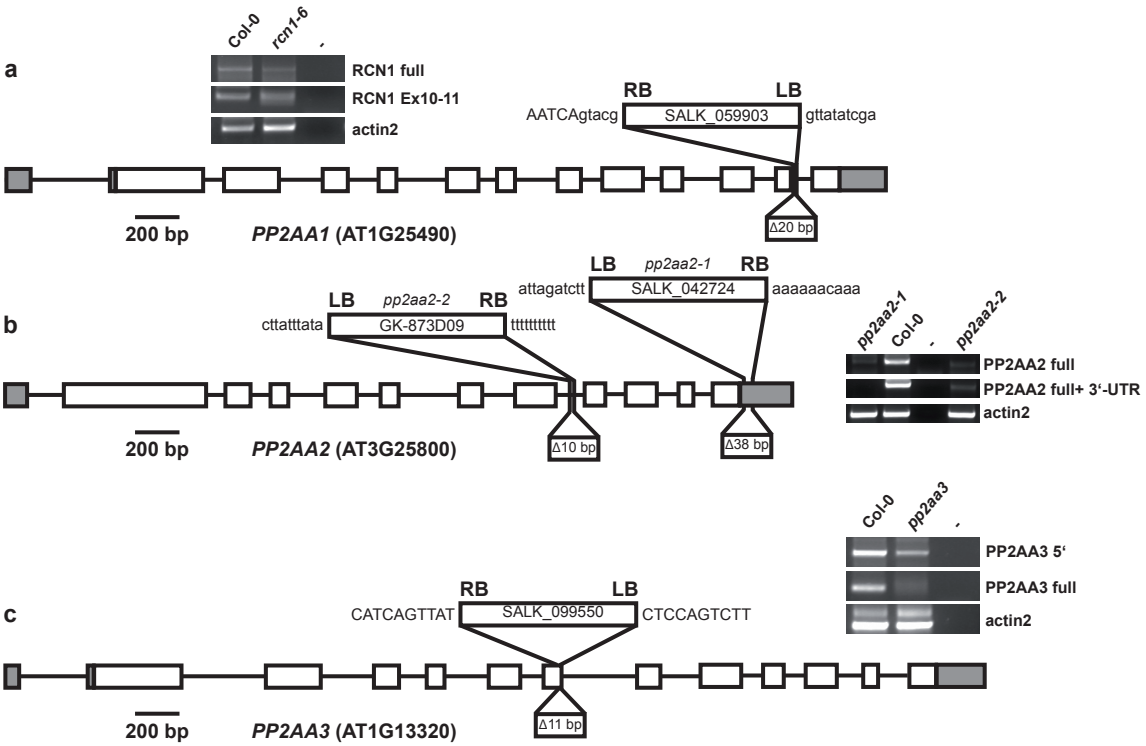

Figure S6. Genomic Maps of PP2AAs and *pp2aa* T-DNA lines. Genomic map of PP2AA1 (RCN1) (**a**), PP2AA2 (**b**) and PP2AA3 (**c**) and respective RT-PCR analyses. Exons and introns are indicated by boxes and lines, respectively. Grey boxes represent untranslated exons. The T-DNA lines inserted in the PP2A genes are presented in upper located boxes with indicated locations of left-borders (LB) and right-borders (RB) and flanking genomic sequences. Lower located boxes indicate genomic deletions caused by the respective T-DNA insertion. Each panel also shows RT-PCR analyses of indicated *pp2a* mutants. For RT-PCRs indicated with "full" T-DNA overlapping primers, "5" primers binding upstream of the T-DNA insertion and "3" primers binding downstream of the T-DNA insertion were used. Actin2 was used as cDNA quality control. "-" indicated respective RT-PCR reaction results without cDNA template.

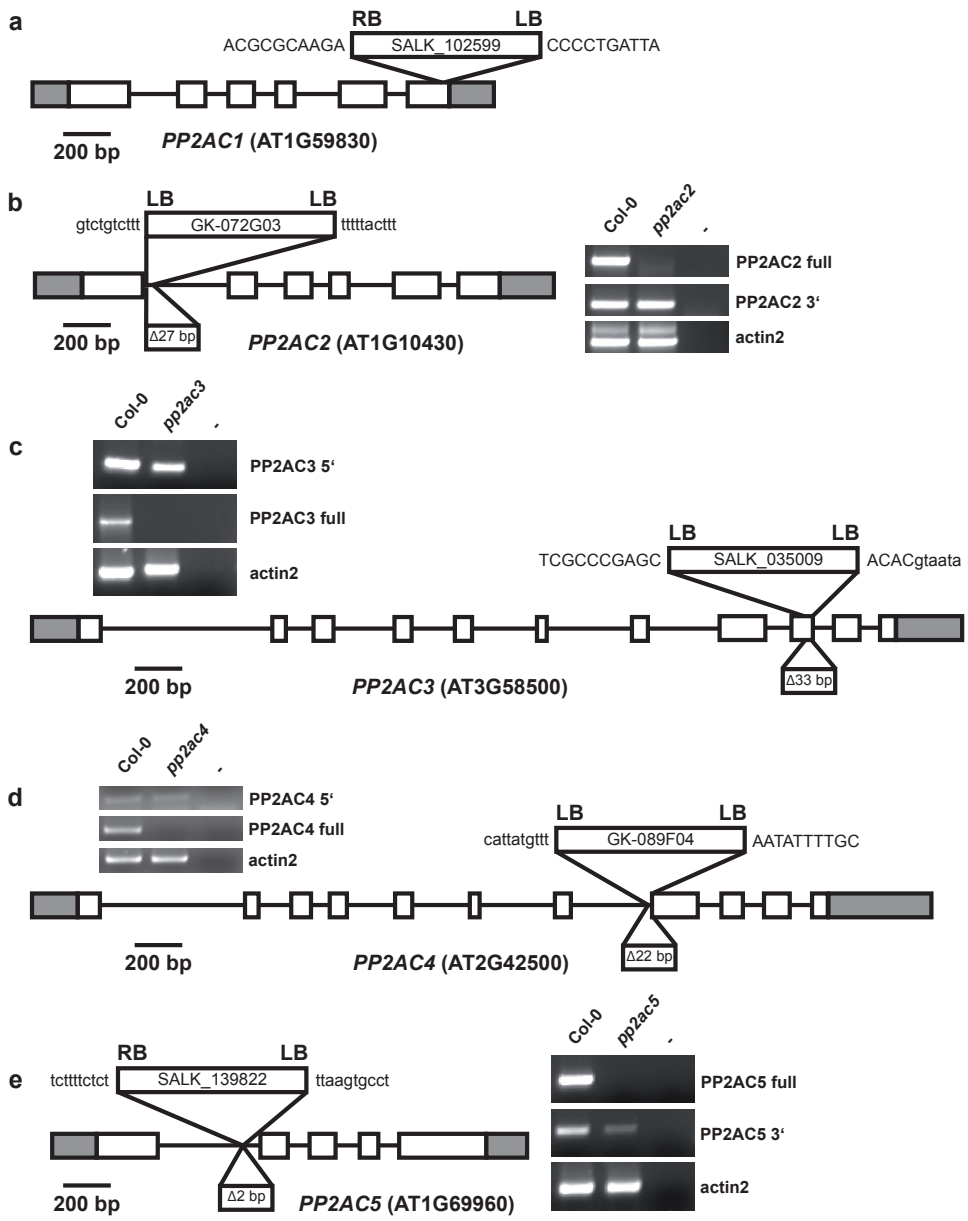

Figure S7. Genomic Maps of PP2ACs and *pp2ac* T-DNA lines. Genomic map of PP2AC1 (**a**), PP2AC2 (**b**) PP2AC3 (**c**) PP2AC4 (**d**) PP2AC5 (**e**) and respective RT-PCR analyses. Exons and introns are indicated by boxes and lines, respectively. Grey boxes represent untranslated exons. The T-DNA lines inserted in the PP2A genes are presented in upper located boxes with indicated locations of left-borders (LB) and right-borders (RB) and flanking genomic sequences. Lower located boxes indicate genomic deletions caused by the respective T-DNA insertion. Each panel also shows RT-PCR analyses of indicated *pp2a* mutants. For RT-PCRs indicated with "full" T-DNA overlapping primers, "5" primers binding upstream of the T-DNA insertion and "3" primers binding downstream of the T-DNA insertion were used. Actin2 was used as cDNA quality control. "-" indicated respective RT-PCR reaction results without cDNA template.

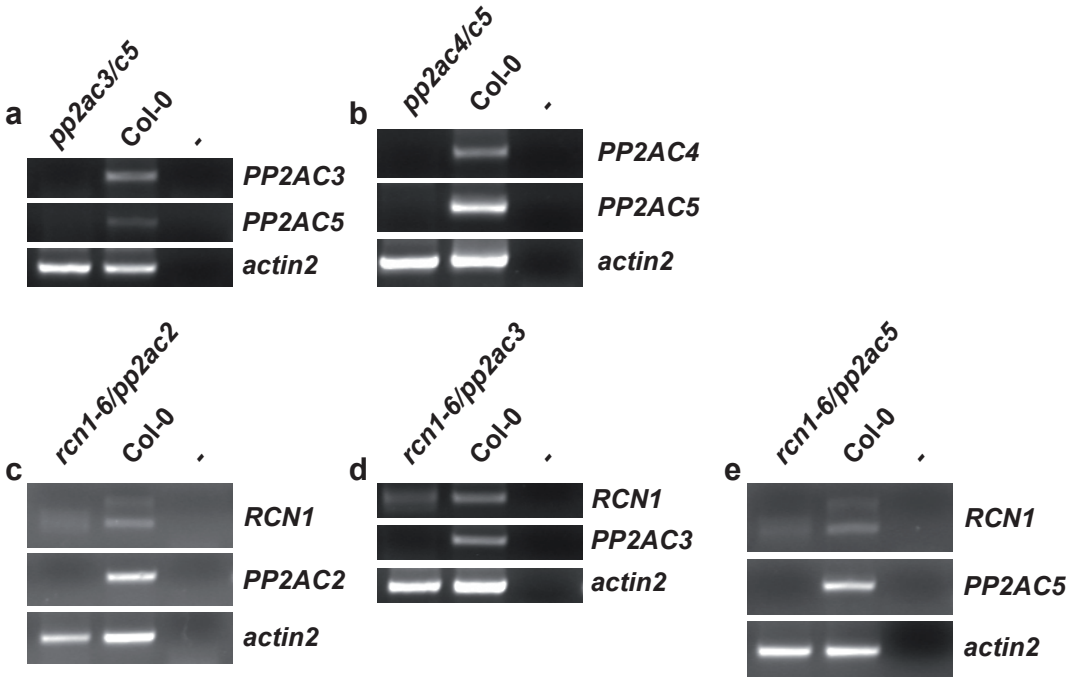

Figure S8. RT-PCRs of *pp2a* double mutant lines. Mutant status of *pp2ac3/pp2ac5* (**a**), *pp2ac4/pp2ac5* (**b**), *rcn1-6/pp2ac2* (**c**), *rcn1-6/pp2ac3* (**d**) and *rcn1-6/pp2ac5* (**c**) was confirmed by RT-PCR analyses. RT-PCR results of the respective PP2A gene are indicated by the PP2A gene name. Actin2 was used as a quality control. "-" indicates result of the RT-PCR reaction without cDNA template.

Table S1. List of oligonucleotides used in this work.

Nr.	AGI Nr.	Gene Name	Primer Name	5'-3'-Sequence	Restric-tion Site	Description
1	-	T-DNA	GABI-LB	cccatttggacgtgaatgt	-	GABI T-DNA left border: 274bp to border sequence
2	-	T-DNA	GABI-RB0	ttgtaaaacgacggccagtgc	-	GABI T-DNA right border: 699bp to border sequence
3	-	T-DNA	SALK_LB1	gtgatggttcacgtagtgg	-	SALK LB T-DNA Primer
4	-	T-DNA	SALK_RB	gagactctaattggataccgag	-	SALK RB T-DNA Primer
5	-	Vector	35S for	gacgcacaatcccactatcc	-	35S Col-PCR and Sequencing Primer
6	-	Vector	BD-for	tcatcggaagagagtag	-	pGBT9.BS
7	-	Vector	BD-rev	taatcataagaaattcgcccg	-	pGBT9.BS
8	-	Vector	LexA_F2	cagcagtcgaggtaagattag	-	Forward XVE sequencing, Colony PCR primer
9	-	Vector	NosT Rev	catctcataaataacgtcatgcattac	-	NosT Col-PCR and Sequencing Primer
10	-	Vector	pACTF2	gcctcctctaacgttcatgat	-	pGAD.GH
11	-	Vector	pACTR	ttgagatggtgcacgatgcacagt	-	pGAD.GH
12	-	Vector	pUBQ10_SeqF	GTCGAATAATTACTCTTCGATTTG	-	pUBQ10 Col-PCR and Sequencing Primer
13	-	Vector	REV	caggaaacagctatgaccatg	-	pKS
14	-	Vector	UNI	gtaaaacgacggccagtgc	-	pKS
15	AT1G10430	PP2AC2	PP2A_C2_Ex1F	GGATGTGAGGACGCTTTGC	-	For Primer for pp2ac2 genotyping (Exon1)
16	AT1G10430	PP2AC2	PP2A_C2_Ex4R	CTGTATCCGATCCAAGCTTC	-	Rev Primer for pp2ac2 genotyping (Exon4)
17	At1g10430	PP2AC2	PP2A_C2_Ex5R	CACACATAGGTCCTTCGTG	-	PP2AC2 reverse Primer for genotyping Exon 5
18	At1g10430	PP2AC2	PP2A_C2_RT5R	GTGTGGAACCTCCTGTATC	-	PP2AC2 RT reverse Primer for genotyping Exon 5-4
19	At1g10430	PP2AC2	PP2A_C2_SpeF	ttt*actagt*ATGCCGTCGAACGGAGATC	Spe I	PP2AC2 forward Primer for genotyping and cloning
20	AT1G10430	PP2AC2	PP2AC2_Ex2F	GATAGACTTACAATCTTACGAG	-	forward primer for genotyping pp2ac2, binds in Exon 2
21	AT1G10430	PP2AC2	PP2AC2_SpeFY	ttt*actagt*gATGCCGTCGAACGGAGATC	Spe I	forward primer for PP2AC2 cloning for YTH assays
22	AT1G10430	PP2AC2	PP2AC2_XmaR	ttt*cccggg*CAAAAAATAATCAGGGGTCTTC	Xma I	Reverse primer for cloning PP2AAC2 for GFP & BiFC
23	AT1G10430	PP2AC2	PP2AC2_XmaRY	ttt*cccggg*TCACAAAAAATAATCAGGGGTCTTC	Xma I	reverse primer for PP2AC2 cloning for YTH assays including stopp
24	AT1G13320	PDF2-PP2AA3	PP2AA3_Ex5F	GAGGCAGAAGTTCGGATAG	-	pp2aa3 Forward Primer for genotyping , Exon 5
25	AT1G13320	PDF2-PP2AA3	PP2AA3_Ex5R	CTATCCGAACTTCTGCCTC	-	reverse primer for genotyping pp2aa3, binds in exon 5
26	AT1G13320	PDF2-PP2AA3	PP2AA3_Ex7R	CGTACATCAGGAAATTCGTC	-	pp2aa3 Reverse Primer for genotyping, Exon 7

Nr.	AGI Nr.	Gene Name	Primer Name	5'-3'-Sequence	Restric-tion Site	Description
27	AT1G13320	PDF2-PP2AA3	PP2AA3_SpeF	ttt*actagt*ATGTCTATGGTTGATGAGCC	Spe I	Forward primer for cloning PP2AA3 for GFP & BiFC
28	At1g13320	PDF2-PP2AA3	PP2AA3_SpeFY	ttt*actagt*gATGTCTATGGTTGATGAGCC	Spe I	forward primer for cloning PP2AA3 (PDF2) into YTH vectors
29	At1g13460	PP2AB'theta	PP2AB'omega_SpeF	ttt*actagt*ATGTGGAAACAGATTCTGAGTA	Spe I	Forward primer for amplification of PP2AB'theta
30	At1g13460	PP2AB'theta	PP2AB'omega_XmaR	ttt*cccggg*CAATGAACTCTTTTGCTTTTGAT	Xma I	Reverse primer for amplification of PP2AB'theta without stopp
31	At1g25490	RCN1	PP2AA1_SpeFY	ttt*actagt*gATGGCTATGGTAGATGAACC	Spe I	forward primer for cloning PP2AA1 (RCN1) into YTH vectors
32	At1g25490	RCN1	PP2AA1_XmaRY	ttt*cccggg*TCAGGATTGTGCTGCTGTG	Xma I	reverse primer for cloning PP2AA1 (RCN1) into YTH vectors with Stop
33	AT1G25490	RCN1	RCN1_Ex10F	CACTACCTACACAGGATGATG	-	forward Primer for genotyping rcn1-6 (Exon10)
34	At1g25490	RCN1	RCN1_SpeF	ttt*actagt*ATGGCTATGGTAGATGAACC	Spe I	Forward Primer to amplify RCN1 for BiFC etc.
35	AT1G25490	RCN1	RCN1_XmaR	ttt*cccggg*GGATTGTGCTGCTGTGGAAC	Xma I	reverse primer for genotyping & cloning RCN1 (non stop)
36	AT1G25490; AT3G25800; AT1G13320	PP2AA1/2/3	PP2AA_1420_SeqR	GCATTGCCCATTCAGGACC	-	Reverse sequencing primer for all 3 PP2AAs
37	At1g51690	PP2ABalpha	PP2ABalpha_SpeF	ttt*actagt*ATGAACGGTGGTGATGAGG	Spe I	Forward primer for amplification of PP2ABalpha
38	At1g51690	PP2ABalpha	PP2ABalpha_XmaR	ttt*cccggg*AGCATAGTACATGTACAAGCTA	Xma I	Reverse primer for amplification of PP2ABalpha without stopp
39	AT1G59830	PP2AC1	PP2AC1_5'UTR_F	ccagagccacctctaacac	-	Forward primer for genotyping pp2ac1 mutant
40	AT1G59830	PP2AC1	PP2AC1_Ex2R	CAGGATCGTAAGTCTGTCC	-	Reverse primer for genotyping pp2ac1 mutant
41	AT1G59830	PP2AC1	PP2AC1_Exon6R	GTTCGACTTGTCTAGGTGC	-	genotyping Primer PP2AC1
42	AT1G59830	PP2AC1	PP2AC1_Exon6R-2	GTAACAGTAGTTCGGTGGAC	-	genotyping primer PP2AC1
43	AT1G59830	PP2AC1	pp2ac1_F	GACTGAGTCTGATCTCAAG	-	genotyping primer
44	AT1G59830	PP2AC1	pp2ac1_R	gaagaggcttctacaaacctg	-	genotyping primer 3'-UTR
45	AT1G59830	PP2AC1	PP2AC1_SpeF	ttt*actagt*ATGCCGTTAAACGGAGATCTC	Spe I	Forward primer for cloning PP2AAC1 for GFP & BiFC
46	AT1G59830	PP2AC1	PP2AC1_SpeFY	ttt*actagt*gATGCCGTTAAACGGAGATCTC	Spe I	forward primer for PP2AC1 cloning for YTH assays
47	AT1G59830	PP2AC1	PP2AC1_XmaR	ttt*cccggg*CAAAAAATAATCAGGGGTCTTG	Xma I	Reverse primer for cloning PP2AAC1 for GFP & BiFC

Nr.	AGI Nr.	Gene Name	Primer Name	5'-3'-Sequence	Restric-tion Site	Description
48	AT1G59830	PP2AC1	PP2AC1_XmaRY	ttt*cccggg*TCACAAAAAATAATCAGGGGTCTTG	Xma I	reverse primer for PP2AC1 cloning for YTH assays including stopp
49	AT1G59830	PP2AC1	pPP2AC1_F	ctgaacagatgattaatctaag	-	Forward primer for genotyping pp2ac1 mutant binds in promoter
50	AT1G69960	PP2AC5	pgPP2AC5_XhoF	ttt*ctcgag*GACATGCTCTTAGTATGGTC	Xho I	forward Primer for amplification of PP2AC5 complementation construct
51	AT1G69960	PP2AC5	pgPP2AC5_XmaR	ttt*cccggg*GATTAGATCTCAGCTCCAGC	Xma I	reverse Primer for amplification of PP2AC5 complementation construct
52	At1g69960	PP2AC5	PP2A_C5_Ex1F	GGAGTGTAAAGCGTTATCTG	-	genomic forward primer, binds in 1st Exon
53	At1g69960	PP2AC5	PP2A_C5_Ex3R	CATATTTCCTCAAACATTCATC	-	PP2AC5 genomic Rev Primer binds in Exon 3
54	At1g69960	PP2AC5	PP2A_C5_RT2F	CTCAAGTGTATGGGTTTTATG	-	RT-PCR forward primer binds in exon 2-3
55	At1g69960	PP2AC5	PP2A_C5_RT4R	CATGTGGAACCTCTTGAATTC	-	PP2AC5 RT Rev Primer spanning Exon 5-4
56	At1g69960	PP2AC5	PP2A_C5_SpeF	ttt*actagt*ATGCCGCCGGCGACCG	Spe I	PP2AC5 Spe For Primer
57	At1g69960	PP2AC5	PP2A_C5_XmaR	ttt*cccggg*CAAAAAATAATCTGGAGTCTTG	Xma I	reverse primer for GFP & BiFC fusion
58	AT1G69960	PP2AC5	PP2AC5_SpeFY	ttt*actagt*gATGCCGCCGGCGACCG	Spe I	forward primer for PP2AC5 cloning for YTH assays
59	AT1G69960	PP2AC5	PP2AC5_XmaRY	ttt*cccggg*TTACAAAAAATAATCTGGAGTCTTG	Xma I	reverse primer for PP2AC5 cloning for YTH assays including stopp
60	AT1G69960	PP2AC5	pPP2AC5_1668F	GGAGACCACAATGCTTCTTTG	-	forward primer for sequencing pgPP2AC5 binds at bp 1668
61	AT1G69960	PP2AC5	pPP2AC5_3252R	CAGATAACGCTTTACACTCC	-	reverse primer for sequencing pgPP2AC5 binds at bp 3252
62	AT1G69960	PP2AC5	pPP2AC5_803F	GTTCCTATAGTGAAGAAATATTG	-	forward primer for sequencing pgPP2AC5 binds at bp 803
63	At2g42500	PP2AC4	PP2A_C4_Ex1F	GGACGCAACCATTGATCTTG	-	For. primer for genotyping pp2ac4 T-DNA insertion; Exon 1
64	At2g42500	PP2AC4	PP2A_C4_Ex3R	GCAAGATCATGGAACTGTCC	-	Rev. primer for genotyping pp2ac4 T-DNA insertion; Exon 3
65	At2g42500	PP2AC4	PP2A_C4_Ex7F	CTTTACAGACCTCTTCGAC	-	For. primer for genotyping pp2ac4 T-DNA insertion; Exon 7
66	At2g42500	PP2AC4	PP2A_C4_XmaR	ttt*cccggg*CAGGAAATAGTCTGGAGTCC	Xma I	Rev. primer for GFP & BiFC fusion and genotyping
67	AT2G42500	PP2AC4	PP2AC4_SpeF	ttt*actagt*ATGGGCGCGAATTCTATTCC	Spe I	Forward primer for cloning PP2AAC4 for GFP & BiFC
68	AT2G42500	PP2AC4	PP2AC4_SpeFY	ttt*actagt*gATGGGCGCGAATTCTATTCC	Spe I	forward primer for PP2AC4 cloning for YTH assays
69	AT2G42500	PP2AC4	PP2AC4_XmaRY	ttt*cccggg*TCACAGGAAATAGTCTGGAGTCC	Xma I	reverse primer for PP2AC4 cloning for YTH assays including stopp

Nr.	AGI Nr.	Gene Name	Primer Name	5'-3'-Sequence	Restric-tion Site	Description
70	AT3G09880	PP2AB'beta	pp2ab'b_F	GAGAATCTCTTCCTTGGAG	-	genotyping primer
71	AT3G09880	PP2AB'beta	PP2AB'beta_SpeF	ttt*actagt*ATGTTTAAGAAAATCATGAAAGG	Spe I	forward primer for amplification of PP2AB'beta
72	AT3G09880	PP2AB'beta	pp2ab'beta_SpeFY	ttt*actagt*gATGTTTAAGAAAATCATGAAAGG	Spe I	cloning primer for yeast
73	AT3G09880	PP2AB'beta	PP2AB'beta_XmaR	ttt*cccggg*GGAAGTGATCATATGATCTTC	Xma I	reverse primer for amplification of PP2AB'beta without stop codon
74	AT3G09880	PP2AB'beta	pp2ab'beta_XmaRY	ttt*cccggg*CTAGGAAGTGATCATATGATC	Xma I	Reverse primer for yeast including stop codon
75	At3g18780	Actin 2	Actin 2 RT For	gtaagagacatcaaggagaagctctc	-	Actin 2 Forw RT-Primer for Transcript analysis
76	At3g18780	Actin 2	Actin 2 RT Rev	ggagatccacatctgctggaatg	-	Actin2 Rev RT-Primer for Transcript analysis
77	At3g21650	PP2AB'zeta	PP2AB'zeta_XhoF	ttt*ctcgag*ATGATCAAACAGATATTTGGGAA	Xho I	Forward primer for amplification of PP2AB'zeta
78	At3g21650	PP2AB'zeta	PP2AB'zeta_XmaR	ttt*cccggg*CGACCCTGTGGACTCAGAG	Xma I	Reverse primer for amplification of PP2AB'zeta without stopp
79	AT3G25800	PDF1-PP2AA2	PP2AA2_3'UTR_R	cgtaccgaggcactctag	-	reverse primer for genotyping pp2aa2 mutants
80	AT3G25800	PDF1-PP2AA2	PP2AA2_Ex11R	CTTGGTTTGCGAAAAACCTG	-	PP2AA2 reverse primer for gentyping
81	AT3G25800	PDF1-PP2AA2	PP2AA2_Ex1F	CAGAAGGCTTTCTACGATCG	-	pp2aa2 Forward Primer for genotyping , Exon 1
82	AT3G25800	PDF1-PP2AA2	PP2AA2_Ex2R	GTTGGACACAATCCTGAGG	-	pp2aa2 Reverse Primer for genotyping, Exon 2
83	AT3G25800	PDF1-PP2AA2	PP2AA2_Ex7F	CTTGTTGCCAGCTATTGTAG	-	PP2AA2 forward primer for gentyping
84	AT3G25800	PDF1-PP2AA2	PP2AA2_Ex9R	GTCATTCGGTAGAGATAGTG	-	Reverse primer for genotyping PP2AA2
85	AT3G25800	PDF1-PP2AA2	PP2AA2_SpeF	ttt*actagt*ATGTCTATGATCGATGAGCC	Spe I	Forward primer for cloning PP2AA2 for GFP & BiFC
86	At3g25800	PDF1-PP2AA2	PP2AA2_SpeFY	ttt*actagt*gATGTCTATGATCGATGAGCC	Spe I	forward primer for cloning PP2AA2 (PDF1) into YTH vectors
87	AT3G25800/AT1G13320	PDF1-PP2AA2/PDF2-PP2AA3	PP2AA2/3_XmaR	ttt*cccggg*GCTAGACATCATCACATTGTC	Xma I	Reverse primer for cloning PP2AA2 & PP2AA3 for GFP & BiFC without Stopp
88	At3g25800/At1g13320	PDF1-PP2AA2/PDF2-PP2AA3	PP2AA2/3_XmaRY	ttt*cccggg*TTAGCTAGACATCATCACATTG	Xma I	reverse primer for cloning PP2AA2 and A3 (PDF1/2) into YTH vectors with Stop
89	AT3G26020	PP2AB'eta	PP2AB'eta_SpeF	ttt*actagt*ATGTGGAAACAGATTCTAAGTA	Spe I	Spe forward primer for PP2AB'eta
90	AT3G26020	PP2AB'eta	PP2AB'eta_XmaR	ttt*cccggg*TGAAGCCTTTCGCACTCCG	Xma I	Xma reverse primer for PP2AB'eta
91	AT3G26030	PP2AB'delta	pp2ab'delta_SpeFY	ttt*actagt*gATGTTTAAGCAGATACTTGGG	Spe I	cloning primer for yeast
92	At3g26030	PP2AB'delta	PP2AB'delta_XhoF	ttt*ctcgag*ATGTTTAAGCAGATACTTGGG	Xho I	Forward primer for amplification of PP2AB'delta

Nr.	AGI Nr.	Gene Name	Primer Name	5'-3'-Sequence	Restric-tion Site	Description
93	At3g26030	PP2AB'delta	PP2AB'delta_XmaR	ttt*cccggg*CTTCGCCATTGAAGCAACAATC	Xma I	Reverse primer for amplification of PP2AB'delta without stopp
94	AT3G26030	PP2AB'delta	pp2ab'delta_XmaRY	ttt*cccggg*TTACTTCGCCATTGAAGCAAC	Xma I	Reverse primer for yeast including stop codon
95	AT3G54930	PP2AB'-epsilon	PP2AB'epsilon_SpeF	ttt*actagt*ATGTTCAACAAAATCATAAAACTG	Spe I	Spe forward primer for PP2AB'epsilon
96	AT3G54930	PP2AB'-epsilon	PP2AB'epsilon_XmaR	ttt*cccggg*GTTAGCAGCTAGAGAAGCAG	Xma I	Xma reverse primer for PP2AB'epsilon
97	At3g58500	PP2AC3	PP2A_C3_Ex8F	GAACTTTGATCGGGTTCAAG	-	PP2AC3 genomic For Primer binds in Exon 8
98	At3g58500	PP2AC3	PP2A_C3_RT1F	CGAGCAACAGGTCAGAGC	-	PP2AC3 RT For Primer spanning Exon 1-2
99	At3g58500	PP2AC3	PP2A_C3_RT8R	GACTCCACCAAGGCTGTC	-	PP2AC3 RT-PCR reverse primer spanning exon 7-8
100	At3g58500	PP2AC3	PP2A_C3_XmaR	ttt*cccggg*AAGGAAATAGTCAGGTGTCC	Xma I	PP2AC3 Xma Rev Primer without Stop
101	AT3G58500	PP2AC3	PP2AC3_SpeF	ttt*actagt*ATGGGCGCGAATTCGCTTC	Spe I	Forward primer for cloning PP2AAC3 for GFP & BiFC
102	AT3G58500	PP2AC3	PP2AC3_SpeFY	ttt*actagt*gATGGGCGCGAATTCGCTTC	Spe I	forward primer for PP2AC3 cloning for YTH assays
103	AT3G58500	PP2AC3	PP2AC3_XmaRY	ttt*cccggg*TCAAAGGAAATAGTCAGGTGTCC	Xma I	reverse primer for PP2AC3 cloning for YTH assays including stopp
104	At4g15415	PP2AB'-gamma	PP2AB'gamma_SpeF	ttt*actagt*ATGATCAAACAGATATTTGGGAA	Spe I	Forward primer for amplification of PP2AB'gamma
105	At4g15415	PP2AB'-gamma	PP2AB'gamma_XmaR	ttt*cccggg*ACTACCCGAAGTTTTACCGG	Xma I	Reverse primer for amplification of PP2AB'gamma without stopp
106	AT5G03470	PP2AB'alpha	pp2ab'alpha_Ex1/2Fa	CTCAGTAGCTCTAATTTTCAGGTTGCAGAACGAGCTCTGTTC	-	Cloning primer pp2ab'alpha from gDNA
107	AT5G03470	PP2AB'alpha	pp2ab'alpha_Ex1/2Ra	GAACAGAGCTCGTTCTGCAACCTGAAAATTAGAGCTACTGAG	-	Cloning primer pp2ab'alpha from gDNA
108	AT5G03470	PP2AB'alpha	pp2ab'alpha_Ex1F	GAGCAGGGAAGCTCACTG	-	Genotyping primer
109	AT5G03470	PP2AB'alpha	pp2ab'alpha_Ex1Fb	CAGGTAGGTCAGGTCCTG	-	forward genotyping primer pp2ab'alpha binds in exon 1
110	AT5G03470	PP2AB'alpha	pp2ab'alpha_Ex2R	GTTCCACAAGAACAGAGCTC	-	Genotyping primer
111	AT5G03470	PP2AB'alpha	PP2AB'alpha_SpeF	ttt*actagt*ATGTTTAAGAAGATCATGAAAGG	Spe I	forward primer for amplification of PP2AB'alpha
112	AT5G03470	PP2AB'alpha	pp2ab'alpha_SpeFY	ttt*actagt*gATGTTTAAGAAGATCATGAAAGG	Spe I	cloning primer for yeast
113	AT5G03470	PP2AB'alpha	PP2AB'alpha_XmaR	ttt*cccggg*AGAAGTGATCATAGGATCTTC	Xma I	reverse primer for amplification of PP2AB'alpha without stop codon
114	AT5G03470	PP2AB'alpha	pp2ab'alpha_XmaRY	ttt*cccggg*CTAAGAAGTGATCATAGGATC	Xma I	Reverse primer for yeast including stop codon
115	AT5G59720	HSP18.2	HSP_Ter_EcoR	ttt*GAATTC*cttatctttaatcatattccatag	Eco RI	reverse Primer for cloning of HSP18.2 Terminator

Table S2. List of constructs used in this work.

Nr.	AGI Nr.	Gene Name	Promoter Name	Clone Name	Cloned 5'	Cloned 3'	Vector (backbone)	Clone Information
1	-	Vector	pUBQ10	barII-UT-mTn	Xba I/Spe I	Sac I	pGPTVII.Bar	pUBQ10-mTurquoise-MCS2-HSP18.2TerM
2	-	Vector	pUBQ10	barII-UT-mVenus-C	Xba I/Spe I	Sac I	pGPTVII.Bar	pUBQ10-MCS-mVenus-HSPTerM
3	-	Vector	UXVE	barII-UTXVE-mTn	Xba I	Xma I	pGPTVII.Bar	pUBQ10-XVE-mTurquoise-mcs2-HSP18.2T
4	-	Vector	UXVE	barII-UTXVE-mVenusC	Xma I	Eco RI	pGPTVII.Bar	pUBQ10-XVE-mcs-mVenus-HSP18.2T
5	-	Vector	p35S	hygII-SPYNE(R)	-	-	pGPTVII.Hyg	eYFP N-Term for N-terminal cloning (BiFC; Waadt et al., 2008)
6	-	Vector	p35S	kanII-SPYCE(MR)	-	-	pGPTVII.Kan	eYFP C-term for N-terminal BiFC cloning (Waadt et al., 2008)
7	-	Vector	-	pGAD.GH	-	-	pGAD.GH	Vector for yeast 2 hybrid analyses (Bartel & Fields, 1997)
8	-	Vector	-	pGBT9.BS	-	-	pGBT9.BS	Vector for yeast 2 hybrid analyses (Bartel & Fields, 1997)
9	-	Vector	-	pKS	-	-	pKS	Cloning vector
10	-	Vector	pUBQ10	pUC-pUBQ10	Hind III	Spe I	pUC	pUBQ10 promoter
11	At1g10430	PP2AC2	pUBQ10	pUC-pUBQ10-PP2AC2-B	Spe I	Xma I	pUC	PP2AC2 with stop codon
12	At1g10430	PP2AC2	-	pGBT9.BS-PP2AC2	Spe I	Xma I	pGBT9.BS	BD-PP2AC2 for YTH assays
13	At1g10430	PP2AC2	p35S	kanII-SPYCE(MR)-PP2AC2-B	Spe I	Xma I	pGPTVII.Kan	YFP C155-PP2AC2 stop for BiFC
14	At1g10430	PP2AC2	pUBQ10	barII-UT-mVenus-PP2AC2-B	Spe I	Xma I	pGPTVII.Bar	mVenus-PP2AC2 stop

Nr.	AGI Nr.	Gene Name	Promoter Name	Clone Name	Cloned 5'	Cloned 3'	Vector (backbone)	Clone Information
15	At1g13320	PDF2-PP2AA3	pUBQ10	pUC-pUBQ10-PP2AA3	Spe I	Xma I	pUC	PP2AA3 without stop for GFP & BiFC analyses
16	At1g13320	PDF2-PP2AA3	pUBQ10	pUC-pUBQ10-PP2AA3_YTH	Spe I	Xma I	pUC	PP2AA3 with stop codon cloned for YTH assays
17	At1g13320	PDF2-PP2AA3	-	pGAD.GH-PP2AA3	Spe I	Xma I	pGAD.GH	PP2AA3 for YTH assays
18	At1g13320	PDF2-PP2AA3	-	pGBT9.BS-PP2AA3	Spe I	Xma I	pGBT9.BS	PP2AA3 for yeast two hybrid assays
19	At1g13320	PDF2-PP2AA3	pUBQ10	barII-UT-mT-PP2AA3	Spe I	Xma I	pGPTVII.Bar	mTurquoise-PP2AA3 for localization analyses
20	At1g13320	PDF2-PP2AA3	pUBQ10	barII-UT-PP2AA3-mVenus	Spe I	Xma I	pGPTVII.Bar	PP2AA3-mVenus for localization analyses
21	At1g13320	PDF2-PP2AA3	p35S	hygII-SPYNE(R)-PP2AA3	Spe I	Xma I	pGPTVII.Hyg	eYFP N173-PP2AA3
22	At1g13320	PDF2-PP2AA3	p35S	kanII-SPYCE(MR)-PP2AA3	Spe I	Xma I	pGPTVII.Kan	eYFP C-terminus-PP2AA3 without stop codon for BiFC analyses
23	At1g13460	PP2AB'-theta	-	pUNI51-PP2AB'theta	-	-	pUNI51	ABRC stock U85787
24	At1g13460	PP2AB'-theta	pUBQ10	pUC-pUBQ10-PP2AB'theta	Spe I	Xma I	pUC	PP2AB'theta cloned into pUC vector for FP & BiFC cloning without Stopp codon
25	At1g13460	PP2AB'-theta	pUBQ10	barII-UT-mT-PP2AB'theta	Spe I	Xma I	pGPTVII.Bar	mTurquoise-PP2AB'theta subcloned into plant vector for localization studies
26	At1g13460	PP2AB'-theta	pUBQ10	barII-UT-PP2AB'theta-mVenus	Spe I	Xma I	pGPTVII.Bar	PP2AB'theta -mVenus subcloned into plant vector for localization studies
27	At1g25490	RCN1	pUBQ10	pUC-pUBQ10-RCN1	Spe I	Xma I	pUC	RCN1 without Stop for FP & BiFC fusion

Nr.	AGI Nr.	Gene Name	Promoter Name	Clone Name	Cloned 5'	Cloned 3'	Vector (backbone)	Clone Information
28	At1g25490	RCN1	pUBQ10	pUC-pUBQ10-PP2AA1-HFY	Spe I	Xma I	pUC	PP2AA1 (RCN1) cloned for YTH frameshift in %' and Stop
29	At1g25490	RCN1	-	pGAD.GH-PP2AA1	Spe I	Xma I	pGAD.GH	RCN1 for YTH experiments
30	At1g25490	RCN1	-	pGBT9.BS-RCN1	Spe I	Xma I	pGBT9.BS	RCN1 for yeast two hybrid assays
31	At1g25490	RCN1	pUBQ10	barII-UT-mT-RCN1	Spe I	Xma I	pGPTVII.Bar	mTurquoise-RCN1 for localization analyses
32	At1g25490	RCN1	pUBQ10	barII-UT-RCN1-mVenus	Spe I	Xma I	pGPTVII.Bar	RCN1-mVenus for localization analyses
33	At1g25490	RCN1	p35S	hygII-SPYNE(R)-RCN1	Spe I	Xma I	pGPTVII.Hyg	eYFP N-term-RCN1 for BiFC experiments
34	At1g25490	RCN1	p35S	kanII-SPYCE(MR)-RCN1	Spe I	Xma I	pGPTVII.Kan	eYFP C-terminus-RCN1 without stop codon for BiFC analyses
35	At1g51690	PP2AB-alpha	pUBQ10	pUC-pUBQ10-PP2ABalpha	Spe I	Xma I	pUC	PP2ABalpha for FP and BiFC fusion
36	At1g51690	PP2AB-alpha	pUBQ10	barII-UT-mT-PP2ABalpha	Spe I	Xma I	pGPTVII.Bar	mTurquoise-PP2ABalpha
37	At1g51690	PP2AB-alpha	pUBQ10	barII-UT-PP2ABalpha-mVenus	Spe I	Xma I	pGPTVII.Bar	PP2ABalpha-mVenus
38	AT1G59830	PP2AC1	pUBQ10	pUC-pUBQ10-PP2AC1-B	Spe I	Xma I	pUC	PP2AC1 with stop codon
39	AT1G59830	PP2AC1	-	pGBT9.BS-PP2AC1	Spe I	Xma I	pGBT9.BS	BD-PP2AC1 for YTH assays
40	AT1G59830	PP2AC1	pUBQ10	barII-UT-mVenus-PP2AC1-B	Spe I	Xma I	pGPTVII.Bar	mVenus-PP2AC1 stop
41	AT1G59830	PP2AC1	p35S	kanII-SPYCE(MR)-PP2AC1-B	Spe I	Xma I	pGPTVII.Kan	YFP C155-PP2AC1 stop for BiFC
42	At1g69960	PP2AC5	pUBQ10	pUC-pUBQ10-PP2AC5	Spe I	Xma I	pUC	PP2AC5 without Stopp cloned for BiFC and GFP analyses
43	At1g69960	PP2AC5	pUBQ10	pUC-pUBQ10-PP2AC5-B	Spe I	Xma I	pUC	PP2AC5 with stop codon

Nr.	AGI Nr.	Gene Name	Promoter Name	Clone Name	Cloned 5'	Cloned 3'	Vector (backbone)	Clone Information
44	At1g69960	PP2AC5	-	pGBT9.BS-PP2AC5	Spe I	Xma I	pGBT9.BS	BD-PP2AC5 for YTH assays
45	At1g69960	PP2AC5	pPP2AC5	barII-pgPP2AC5	Xho I	Xma I	pGPTVII.Bar	complementation construct for PP2AC5
46	At1g69960	PP2AC5	pUBQ10	barII-UT-PP2AC5-mVenus	Spe I	Xma I	pGPTVII.Bar	PP2AC5-mVenus
47	At1g69960	PP2AC5	pUBQ10	barII-UT-mVenus-PP2AC5-B	Spe I	Xma I	pGPTVII.Bar	mVenus-PP2AC5 stop
48	At1g69960	PP2AC5	p35S	kanII-SPYCE(MR)-PP2AC5-B	Spe I	Xma I	pGPTVII.Kan	YFP C155-PP2AC5 stop for BiFC
49	At2g42500	PP2AC4	pUBQ10	pUC-pUBQ10-PP2AC4	Spe I	Xma I	pUC	PP2AC4 without Stopp cloned for BiFC and GFP analyses
50	At2g42500	PP2AC4	pUBQ10	pUC-pUBQ10-PP2AC4-B	Spe I	Xma I	pUC	PP2AC4 with stop codon
51	At2g42500	PP2AC4	p35S	kanII-SPYCE(MR)-PP2AC4-B	Spe I	Xma I	pGPTVII.Kan	YFP C155-PP2AC4 stop for BiFC
52	At2g42500	PP2AC4	pUBQ10	barII-UT-PP2AC4-mVenus	Spe I	Xma I	pGPTVII.Bar	PP2AC4-mVenus
53	At2g42500	PP2AC4	pUBQ10	barII-UT-mVenus-PP2AC4-B	Spe I	Xma I	pGPTVII.Bar	mVenus-PP2AC4 stop
54	At2g42500	PP2AC4	-	pGBT9.BS-PP2AC4	Spe I	Xma I	pGBT9.BS	BD-PP2AC4 for YTH assays
55	AT3G09880	PP2AB'beta	pUBQ10	pUC-pUBQ10-PP2AB'beta	Spe I	Xma I	pUC	PP2AB'beta for FP and BiFC fusion
56	AT3G09880	PP2AB'beta	pUBQ10	barII-UT-mT-PP2AB'beta	Spe I	Xma I	pGPTVII.Bar	mTurquoise-PP2AB'beta
57	AT3G09880	PP2AB'beta	pUBQ10	barII-UT-PP2AB'beta-mVenus	Spe I	Xma I	pGPTVII.Bar	PP2AB'beta-mVenus
58	At3g21650	PP2AB'zeta	pUBQ10	pUC-pUBQ10-PP2AB'zeta	Xho I	Xma I	pUC	PP2AB'zeta for FP and BiFC fusion
59	At3g21650	PP2AB'zeta	pUBQ10	barII-UT-mT-PP2AB'zeta	Xho I	Xma I	pGPTVII.Bar	mTurquoise-PP2AB'zeta
60	At3g21650	PP2AB'zeta	pUBQ10	barII-UT-PP2AB'zeta-mVenus	Xho I	Xma I	pGPTVII.Bar	PP2AB'zeta-mVenus
61	At3g25800	PDF1-PP2AA2	pUBQ10	pUC-pUBQ10-PP2AA2	Spe I	Xma I	pUC	PP2A without stop for GFP & BiFC analyses

Nr.	AGI Nr.	Gene Name	Promoter Name	Clone Name	Cloned 5'	Cloned 3'	Vector (backbone)	Clone Information
62	At3g25800	PDF1-PP2AA2	pUBQ10	pUC-pUBQ10-PP2AA2-HFY	Spe I	Xma I	pUC	PP2AA2 cloned for YTH assays, frameshift in 5' & Stop
63	At3g25800	PDF1-PP2AA2	-	pGAD.GH-PP2AA2	Spe I	Xma I	pGAD.GH	PP2AA2 for YTH experiments
64	At3g25800	PDF1-PP2AA2	-	pGBT9.BS-PP2AA2	Spe I	Xma I	pGBT9.BS	PP2AA2 for yeast two hybrid assays
65	At3g25800	PDF1-PP2AA2	pUBQ10	barII-UT-mT-PP2AA2	Spe I	Xma I	pGPTVII.Bar	mTurquoise-PP2AA2 for localization analyses
66	At3g25800	PDF1-PP2AA2	pUBQ10	barII-UT-PP2AA2-mVenus	Spe I	Xma I	pGPTVII.Bar	PP2AA2-mVenus for localization analyses
67	At3g25800	PDF1-PP2AA2	p35S	hygII-SPYNE(R)-PP2AA2	Spe I	Xma I	pGPTVII.Hyg	eYFP N173-PP2AA2
68	At3g25800	PDF1-PP2AA2	p35S	kanII-SPYCE(MR)-PP2AA2	Spe I	Xma I	pGPTVII.Kan	eYFP C-terminus-PP2AA2 without stop codon for BiFC analyses
69	AT3G26020	PP2AB'eta	-	pUNI51-PP2AB'eta	-	-	pUNI51	ABRC stock U12213
70	AT3G26020	PP2AB'eta	pUBQ10	pUC-pUBQ10-PP2AB'eta	Spe I	Xma I	pUC	PP2AB'eta without stop codon for FP & BiFC fusion
71	AT3G26020	PP2AB'eta	UXVE	barII-UTXVE-mT-PP2AB'eta	Spe I	Xma I	pGPTVII.Bar	beta-Estradiol inducible mTurquoise-PP2AB'eta
72	AT3G26020	PP2AB'eta	UXVE	barII-UTXVE-PP2AB'eta-mVenus	Spe I	Xma I	pGPTVII.Bar	beta-Estradiol inducible PP2AB'eta-mVenus
73	At3g26030	PP2AB'-delta	-	pUNI51-PP2AB'delta	-	-	pUNI51	ABRC stock U18933
74	At3g26030	PP2AB'-delta	pUBQ10	pUC-pUBQ10-PP2AB'delta	Xho I	Xma I	pUC	PP2AB'delta for FP and BiFC fusion
75	At3g26030	PP2AB'-delta	pUBQ10	barII-UT-mT-PP2AB'delta	Xho I	Xma I	pGPTVII.Bar	mTurquoise-PP2AB'delta
76	At3g26030	PP2AB'-delta	pUBQ10	barII-UT-PP2AB'delta-mVenus	Xho I	Xma I	pGPTVII.Bar	PP2AB'delta-mVenus
77	AT3G54930	PP2AB'-epsilon	-	pUNI51-PP2AB'epsilon	-	-	pUNI51	ABRC stock U61948
78	AT3G54930	PP2AB'-epsilon	pUBQ10	pUC-pUBQ10-PP2AB'epsilon	Spe I	Xma I	pUC	PP2AB'epsilon without stop codon for FP & BiFC fusion

Nr.	AGI Nr.	Gene Name	Promoter Name	Clone Name	Cloned 5'	Cloned 3'	Vector (backbone)	Clone Information
79	AT3G54930	PP2AB'-epsilon	UXVE	barII-UTXVE-mT-PP2AB'epsilon	Spe I	Xma I	pGPTVII.Bar	beta-Estradiol inducible mTurquoise-PP2AB'epsilon
80	AT3G54930	PP2AB'-epsilon	UXVE	barII-UTXVE-PP2AB'epsilon-mVenus	Spe I	Xma I	pGPTVII.Bar	beta-Estradiol inducible PP2AB'epsilon-mVenus
81	At3g58500	PP2AC3	pUBQ10	pUC-pUBQ10-PP2AC3	Spe I	Xma I	pUC	PP2AC3 without Stopp cloned for BiFC and GFP analyses
82	At3g58500	PP2AC3	pUBQ10	pUC-pUBQ10-PP2AC3-B	Spe I	Xma I	pUC	PP2AC3 with stop codon
83	At3g58500	PP2AC3	-	pGBT9.BS-PP2AC3	Spe I	Xma I	pGBT9.BS	BD-PP2AC3
84	At3g58500	PP2AC3	pUBQ10	barII-UT-mVenus-PP2AC3-B	Spe I	Xma I	pGPTVII.Bar	mVenus-PP2AC3 stop
85	At3g58500	PP2AC3	pUBQ10	barII-UT-PP2AC3-mVenus	Spe I	Xma I	pGPTVII.Bar	PP2AC3-mVenus for localization analyses
86	At3g58500	PP2AC3	p35S	kanII-SPYCE(MR)-PP2AC3-B	Spe I	Xma I	pGPTVII.Kan	YFP C155-PP2AC3 stop for BiFC
87	At4g15415	PP2AB'-gamma	-	pUNI51-PP2AB'gamma	-	-	pUNI51	ABRC stock S69317
88	At4g15415	PP2AB'-gamma	pUBQ10	pUC-pUBQ10-PP2AB'gamma	Spe I	Xma I	pUC	PP2AB'gamma for FP and BiFC fusion
89	At4g15415	PP2AB'-gamma	pUBQ10	barII-UT-mT-PP2AB'gamma	Spe I	Xma I	pGPTVII.Bar	mTurquoise-PP2AB'gamma
90	At4g15415	PP2AB'-gamma	pUBQ10	barII-UT-PP2AB'gamma-mVenus	Spe I	Xma I	pGPTVII.Bar	PP2AB'gamma-mVenus
91	At4g26080	ABI1	p35S	kanII-SPYCE(MR)-ABI1	Spe I	Xho I	pGPTVII.Kan	ABI1 for BiFC
92	At4g33950	OST1	pUBQ10	barII-pUBQ10-OST1_HF	Spe I	Xma I	pGPTVII.Bar	OST1_HF for Co-IP experiments with Hellfire Tag
93	At4g33950	OST1	p35S	hygII-SPYNE(R)-OST1	Spe I	Xma I	pGPTVII.Hyg	eYFP N-term-OST1 without Stop for BiFC experiments
94	AT5G03470	PP2AB'-alpha	pUBQ10	pUC-pUBQ10-PP2AB'alpha	Spe I	Xma I	pUC	PP2AB'alpha without stop for FP & BiFC

Nr.	AGI Nr.	Gene Name	Promoter Name	Clone Name	Cloned 5'	Cloned 3'	Vector (backbone)	Clone Information
95	AT5G03470	PP2AB'-alpha	pUBQ10	barII-UT-mT-PP2AB'alpha	Spe I	Xma I	pGPTVII.Bar	mTurquoise-PP2AB'alpha without stop codon for localization experiments
96	AT5G03470	PP2AB'-alpha	UXVE	barII-UTXVE-mT-PP2AB'alpha	Spe I	Xma I	pGPTVII.Bar	beta-Estradiol inducible mTurquoise-PP2AB'alpha
97	AT5G03470	PP2AB'-alpha	UXVE	barII-UTXVE-PP2AB'alpha-mVenus	Spe I	Xma I	pGPTVII.Bar	beta-Estradiol inducible PP2AB'alpha-mVenus
98	AT5G03470	PP2AB'-alpha	p35S	kanII-SPYCE(MR)-PP2AB'alpha	Spe I	Xma I	pGPTVII.Kan	eYFP C-terminus-PP2AB'alpha without stop codon for BiFC analyses